Available online at www.sciencedirect.com
ScienceDirect
Journal of Solid State Chemistry 180 (2007) 636–653
JOURNAL OF SOLID STATE CHEMISTRY
www.elsevier.com/locate/jssc

Ternary rare earth and actinoid transition metal carbides viewed as carbometalates

Enkhtsetseg Dashjav[a], Guido Kreiner[a], Walter Schnelle[a], Frank R. Wagner[a], Rüdiger Kniep[a,*], Wolfgang Jeitschko[b]

[a]*Max-Planck-Institut für Chemische Physik fester Stoffe, Nöthnitzer Straße 40, D-01187 Dresden, Germany*
[b]*Institut für Anorganische und Analytische Chemie, Universität Münster, Wilhelm-Klemm-Straße 8, D-48149 Münster, Germany*

Received 2 October 2006; received in revised form 8 November 2006; accepted 13 November 2006
Available online 30 November 2006

Abstract

Ternary carbides $A_xT_yC_z$ (A = rare earth metals and actinoids; T = transition metals) with monoatomic species C^{4-} as structural entities are classified according to the criteria (i) metal to carbon ratio, (ii) coordination number of the transition metal by carbon atoms, and (iii) the dimensionality of the anionic network $[T_yC_z]^{n-}$. Two groups are clearly distinguishable, depending on the metal to carbon ratio. Those where this ratio is equal to or smaller than 2 may be viewed as carbometalates, thus extending the sequence of complex anions from fluoro-, oxo-, and nitridometalates to carbometalates. The second group, metal-rich carbides with metal to carbon ratios equal to or larger than 4 is better viewed as typical intermetallics (''interstitial carbides''). The chemical bonding properties have been investigated by analyzing the Crystal Orbital Hamilton Population (COHP). The chemical bonding situation with respect to individual T–C bonds is similar in both classes. The main difference is the larger number of metal–metal bonds in the crystal structures of the metal-rich carbides.

Keywords: Carbides; Carbometalates; Rare earth metals; Transition metals; Crystal structure; Chemical bonding

1. Introduction

In the past decades, a large number of investigations were focused on the synthesis, structural characterization and properties of ternary carbides $A_xT_yC_z$ (A = rare earth metals, thorium, uranium; T = transition metals). Almost 60 different structure types have been reported for such ternary carbides including some 20 with monoatomic species C^{4-} as structural units. The other carbides contain carbon pairs C_2 or occasionally linear C_3 units. In this paper, we discuss the concept of *carbometalates*, which is useful for the classification of those structure types containing monoatomic C^{4-} species.[1]

We start with a brief review of the structural chemistry of the carbides $A_xT_yC_z$ with isolated carbon atoms. Those with high carbon content are classified as carbometalates, and in reviewing their structural chemistry, we emphasize the near-neighbor coordinations of the transition metal atoms and the dimensionality of the complex transition metal carbon polyanions $[T_yC_z]^{n-}$. A central part of the paper is the analysis of chemical bonding. This is carried out on the basis of band structure calculations using the Crystal Orbital Hamilton Population (COHP) method. The results of these calculations are then used to examine chemical bonding in carbometalates containing the more or less covalent complex polyanions as compared to metal-rich carbides. In addition, the carbometalates are then compared to the nitridometalates and finally they are also related to oxo- and fluorometalates.

*Corresponding author. Fax: +49 351 46 46 30 02.
E-mail addresses: Kniep@cpfs.mpg.de (R. Kniep), jeitsch@uni-muenster.de (W. Jeitschko).

[1]For counting electrons we use oxidation numbers, where a bonding electron of a more or less covalent bond is counted at that atom with the higher electronegativity. Thus, oxidation numbers (roman numerals, 0, see Nomenclature of Inorganic Chemistry, IUPAC Recommendations 2005) and likewise the ionic charges do not necessarily imply ionic bonding, a frequently encountered misunderstanding.

0022-4596/$ - see front matter © 2006 Elsevier Inc. All rights reserved.
doi:10.1016/j.jssc.2006.11.019

2. Structural chemistry of carbides with isolated carbon atoms

The crystal structure types of the ternary carbides $A_xT_yC_z$ containing isolated carbon atoms are listed in Table 1. They are arranged according to increasing metal to carbon atom ratios $(x+y)/z$. Also given are some representatives, the idealized formulae with oxidation numbers enclosing the polyanionic transition metal carbon substructure in brackets, the coordination polyhedra of the transition metals with respect to the carbon atoms, the dimensionality of the polyanionic substructure, and the bibliographical references. Some representative structural data of these compounds are listed in Table 2.

Two groups of carbides with monoatomic carbon species are clearly distinguishable. In Table 1 they are labelled as *carbometalates* and *metal-rich carbides*, respectively. The group of compounds classified as carbometalates contains complex anions $[T_yC_z]^{n-}$ where the carbon atoms are more or less covalently bonded to the transition metal atoms. These polyanions occur as discrete "zero-dimensional" units, anionic chains, layers, and three-dimensional networks, respectively. For carbometalates, the metal atom to carbon atom ratios $(x+y)/z$ range from 1 to 2. The carbon positions in the carbometalates are usually fully occupied, and thus the compositions of these compounds are well defined. The coordination numbers (CN) of the transition elements with respect to the carbon atoms are small, ranging from 2 to 5. Frequently the oxidation states of the transition metals can readily be assigned knowing the crystal structure of these carbometalates, since by definition the isolated carbon atoms are counted as C^{4-}, whereas the rare earth metals were assumed to be essentially in the A^{III} valence state. This point is discussed in more detail below.

The second group of carbides $A_xT_yC_z$ with monoatomic species C^{4-} as structural units may be classified as *metal-rich carbides*. Here, the metal atoms are greater in number, the ratio $(x+y)/z$ being between 4 and 16. These carbides may be viewed as interstitial carbides, where the carbon atoms frequently are found to not fully occupy their positions, although the homogeneity ranges corresponding to the statistical occupation of the carbon sites have rarely been investigated. In these metal-rich carbides some of the transition metal atoms are not even coordinated by any carbon atom. Due to the dominating metal–metal interactions and the fact that some of the carbon sites are vacant, it is not appropriate to single out discrete transition metal carbon polyanions and the assignment of oxidation numbers for the transition metal atoms is impractical.

We will now discuss the various crystal structures listed in Table 1 in more detail. It is most remarkable that the positions of all metal atoms in the compounds listed as carbometalates correspond to those of a body-centered cubic (bcc) structure. This has been recognized earlier for the structures of those compounds known for some time [3,14] and this is also true for the most recent members of this list, i.e. $Er_2Mo_2C_3$ [9], Pr_2MoC_2 [12], and $Pr_2Mo_2C_3$ [11]. The differences between these 11 structure types arise through the various possibilities of atomic order of the A and T atoms on the bcc positions and through the ordered arrangement of the carbon atoms in the (distorted) octahedral voids of the bcc-like structures. There are six heavily distorted octahedral voids per two metal positions of a bcc (W type) structure, and most of them remain unoccupied in these 11 carbometalate structures.

2.1. Compounds with metal/carbon ratios $(x+y)/z$ of 1 and 1.25

The first four compounds listed in Table 1 all contain uranium as the most electropositive element: $UMoC_2$ [1], $U_5Re_3C_8$ [3], UCr_4C_4 [4], and UW_4C_4 [5,6]. They have the lowest metal contents of all compounds listed, with metal to carbon ratios $(x+y)/z$ of 1 or 1.25, respectively. For these four uranium compounds oxidation numbers for the metal atoms are not given in Table 1. By definition, the isolated carbon atoms with the highest electronegativity in their respective compounds carry the ionic charge of 4−. However, it is difficult to assign counterbalancing positive charges to the metal atoms, since the oxidation numbers of the uranium atoms are not known. Nevertheless, at least for the $UMoC_2$-type series $AMoC_2$ and AWC_2, where A is a rare earth metal, such assignments can be made, since the rare earth elements A forming these compounds are known to prefer the valence state A^{III}. Thus, for instance with A = yttrium, one can assign oxidation numbers according to the formulae $Y^{III}[Mo^{V}C_2^{-IV}]$ and $Y^{III}[W^{V}C_2^{-IV}]$. In analogy, for the corresponding uranium compound a formula $U^{III}[Mo^{V}C_2^{-IV}]$ looks reasonable, and the ionic charge 3− can be assigned to the corresponding polyanion $[TC_2]$. For the other three structure types—$U_5Re_3C_8$, UCr_4C_4, and UW_4C_4—no isotypic rare earth compounds are known. Thus, in these carbometalates the uranium atoms could be assigned the oxidation number III, as just discussed, or even higher oxidation states. However, magnetic susceptibility data of these three compounds suggest mixed or intermediate valencies III/IV for uranium [39] as frequently observed for intermetallic uranium compounds. Nonetheless, these uranium compounds can be clearly classified as carbometalates because of their low $(x+y)/z$ ratios and their structural similarities to the other carbometalates listed in Table 1.

The compounds $UMoC_2$ and $U_5Re_3C_8$ have the lowest metal content of all the carbides listed in Table 1 with $(x+y)/z$ of 1. Consequently, in these carbometalates the transition metal atoms have the highest carbon coordination with CN = 5. In $UMoC_2$ there is only one crystallographic site for molybdenum, and these Mo atoms have five carbon neighbors forming a distorted trigonal bipyramid. These trigonal bipyramids share corners and edges, thus creating an infinite polyanionic network of composition $^3_\infty[(MoC_2)^{n-}]$ as shown in Fig. 1. In this figure as well as in the following ones (Figs. 2–8) only the carbon

Table 1
Classification of ternary carbides $A_xT_yC_z$ (A = rare earth metals, actinoids, T = transition metals) containing monoatomic species C^{4-} as structural units

Structure type	Representatives	Idealized formula	CP[a]	D[b]	$(x+y)/z$
Carbometalates					
$UMoC_2$	$AMoC_2$ (A = Y, Gd–Tm), AWC_2 (A = Y, Tb–Tm, Pu), UTC_2 (T = V–Mn, Mo, Tc, W, Re) [1,2]	$Y^{III}[Mo^{V}C_2^{-IV}]$[c] $Y^{III}[W^{V}C_2^{-IV}]$ [c)]	5by	$^3_\infty$	1
$U_5Re_3C_8$	$U_5Re_3C_8$ [3]	—	5by, 4s	$^3_\infty$	1
UCr_4C_4	UCr_4C_4 [4]	—	4t	$^3_\infty$	1.25
UW_4C_4	UW_4C_4 [5,6]	—	4t	$^3_\infty$	1.25
$Ho_2Cr_2C_3$	$A_2Cr_2C_3$ (A = Y, Gd–Lu) $Sm_2Mo_2C_3$ [2,7,8]	$Ho_2^{III}[Cr_2^{III}C_3^{-IV}]$	4t	$^2_\infty$	1.33
$Er_2Mo_2C_3$	$A_2Mo_2C_3$ (A = Ce, Gd–Tm, Lu) [9,10]	$Er_2^{III}[Mo_2^{III}C_3^{-IV}]$	4t	$^2_\infty$	1.33
$Pr_2Mo_2C_3$	$Pr_2Mo_2C_3$ [11]	$Pr_2^{III}[Mo_2^{III}C_3^{-IV}]$	4t	$^3_\infty$	1.33
Pr_2MoC_2	A_2MoC_2 (A = Pr, Nd), A_2WC_2 (A = Ce, Pr) [12,13]	$Pr_2^{III}[Mo^{II}C_2^{-IV}]$	4t	$^2_\infty$	1.5
Pr_2ReC_2	A_2ReC_2 (A = Y, Ce–Nd, Sm, Gd–Tm, Lu), A_2OsC_2 (A = Y, Gd–Er) [14,15]	$Pr_2^{III}[Re^{II}C_2^{-IV}]$	31	$^1_\infty$	1.5
U_2IrC_2	Th_2TC_2 (T = Ru, Os, Rh, Ir, Ni, Pt) [16,17]	$Th_2^{IV}[Ni^{0}C_2^{-IV}]$[c]	21	$^0_\infty$	1.5
YCoC	$ACoC$ (A = Y, Gd–Lu) [18,19]	$Y^{III}[Co^{I}C^{-IV}]$	21	$^1_\infty$	2
Mixed					
$La_5Os_3C_{4-x}$	$A_5Os_3C_{4-x}$ (A = La–Nd, Sm) [20]	—	2n	$^1_\infty$	2

Metal-rich carbides Structure type	Representatives	CP and number of C[d]	$(x+y)/z$
Filled Cu_3Au perovskite	Many representatives, e.g., $ThRu_3C$ [21,22]	12co + 2C	4
$LaMn_{11}C_{2-x}$	$AMn_{11}C_{2-x}$ (A = La–Nd, Th) [23], $ThFe_{11}C_{2-x}$ [24]	12i, 12i + 1C, 14FK	~6
$Pr_2Mn_{17}C_{3-x}$	$A_2Mn_{17}C_{3-x}$ (A = La–Nd, Sm, Th) [25]	12i, 12i + 1C, 14FK	~6.3
$Tb_2Mn_{17}C_{3-x}$	$A_2Mn_{17}C_{3-x}$ (A = Y, Gd–Tm, Lu) [26], $A_2Fe_{17}C_{3-x}$ (A = Nd, Tb, Dy, Lu) [27]		
$Ce_2Ni_{22}C_{3-x}$	$A_2Ni_{22}C_{3-x}$ (A = La–Nd, Sm, Gd–Ho) [28–30]	11 + 2C, 12i, 12 + 1C, 13 + 1C, 14FK	~8
$Tm_{11}Ni_{60}C_6$	$A_{11}Ni_{60}C_6$ (A = Y, Dy–Lu) [31–33]	12i, 12i + 1C, 14FK	11.8
$Nd_2Fe_{14}B$	$A_2Fe_{14}C$ (A = Pr, Sm, Gd–Tm, Lu) [34–37]	11 + 1C, 11 + 2C, 12i, 14FK	16

[a]Coordination type polyhedron of T by C with coordination number and polyhedron designated by symbols as proposed in [38]: 5by—trigonal *bipyramid*; 4s—*s*quare planar; 4t—*t*etrahedral; 3l—trigonal p*l*anar; 2l—co*l*linear; 2n—*n*on-collinear.
[b]Dimensionality of the complex anion.
[c]see text.
[d]Coordination type polyhedron of T by M = T, A [38] and number of nearest carbon neighbors: 12co—*c*ubo*c*tahedron; 12i—*i*cosahedron; 14FK—*F*rank-*K*asper polyhedron ; no symbol letter is given in case of irregular polyhedra.

neighbors of each transition metal atom are shown, thus emphasizing the strong T–C bonds and omitting the weak metal–metal interactions. The TC_n polyhedra are shown together with interatomic distances $d(T–C)$. In the corresponding graphs the C–T–C bond angles are indicated.

A distorted trigonal bipyramid of carbon atoms also present as coordination polyhedron around one of the two kinds of rhenium atoms in the crystal structure of $U_5Re_3C_8$, while the other rhenium atom in that compound has a square-planar carbon coordination. Again, an infinite three-dimensional polyanion of the composition $^3_\infty[(Re_3C_8)^{n-}]$ is formed by sharing corners of the ReC_5 and ReC_4 units (Fig. 2).

The other two structure types with uranium as the A component, UCr_4C_4 [4] and UW_4C_4 [5,6], are very similar. UCr_4C_4 has a body-centered tetragonal structure with space group symmetry $I4/m$. UW_4C_4 crystallizes *klassengleich* in the primitive space group $P4/m$ with similar lattice parameters. Thus, while the chromium compound has only one crystallographic site for each atomic species, the number of atomic positions is

Table 2
Structural data of selected ternary carbometalates and metal-rich carbides

Compound	Crystal structure data	Ref.
Carbometalates		
$UMoC_2$	*oP*16, *Pnma*, $a = 561.2$ $b = 324.1$, $c = 1095.6$ pm	[1]
$U_5Re_3C_8$	*tP*32, *P*4/*mbm*, $a = 1131.3$, $c = 330.3$ pm	[3]
UCr_4C_4	*tI*18, *I*4/*m*, $a = 793.6$ $c = 307.5$ pm	[4]
UW_4C_4	*tP*18, *P*4/*m*, $a = 832.8$, $c = 313.5$ pm	[5]
$Ho_2Cr_2C_3$	*mC*14, *C*2/*m*, $a = 1047.0$, $b = 336.5$, $c = 554.0$ pm, $\beta = 106.3°$	[2]
$Y_2Cr_2C_3$	*mC*14, *C*2/*m*, $a = 1047.2$, $b = 339.2$, $c = 554.9$ pm, $\beta = 106.27°$	[7]
$Er_2Mo_2C_3$	*mC*14, *C*2/*m*, $a = 1155.9$, $b = 330.9$, $c = 563.7$ pm, $\beta = 111.3°$	[9]
$Pr_2Mo_2C_3$	*mP*28, $P2_1/n$, $a = 598.0$, $b = 665.2$, $c = 1185.6$ pm, $\beta = 111.6°$	[11]
Pr_2MoC_2	*tP*20, $P4_2/mnm$, $a = 581.3$, $c = 1032.5$ pm	[12]
Pr_2ReC_2	*oP*20, *Pnma*, $a = 665.6$, $b = 534.5$, $c = 1018.4$ pm	[14]
Y_2ReC_2	*oP*20, *Pnma*, $a = 655.7$, $b = 509.5$, $c = 984.4$ pm	[14]
Y_2OsC_2	*oP*20, *Pnma*, $a = 645.0$, $b = 508.9$, $c = 978.0$ pm	[15]
U_2IrC_2	*tI*10, *I*4/*mmm*, $a = 348.0$, $c = 1248.2$ pm	[16]
YCoC	*tP*6, $P4_2/mmc$, $a = 365.0$, $c = 686.4$ pm	[18]
Mixed		
$La_5Os_3C_{4-x}$	*hP*24, $P6_3/mcm$, $a = 919.6$, $c = 673.9$ pm	[20]
Metal-rich carbides		
YRh_3C	*cP*5, $Pm\bar{3}m$, $a = 413.1$ pm	[22]
$LaMn_{11}C_{2-x}$	*tI*56, $I4_1/amd$, $a = 1041.3$, $c = 672.9$ pm, $x = 0.5$	[23]
$Pr_2Mn_{17}C_{3-x}$	*hR*22, $R\bar{3}m$, $a = 887.1$, $c = 1278.3$ pm, $x = 1.23$	[25]
$Tb_2Mn_{17}C_{3-x}$	*hP*50, $P6_3/mmc$, $a = 873.8$, $c = 851.1$ pm, $x = 0.57$	[26]
$Ce_2Ni_{22}C_{3-x}$	*oC*216, *Cmca*, $a = 1137.3$ $b = 1500.4$, $c = 1462.5$ pm, $x = 0.25$	[28]
$Tm_{11}Ni_{60}C_6$	*cI*154, *Im*3*m*, $a = 1245.3$ pm	[31]
$Pr_2Fe_{14}C$	*tP*68, $P4_2/mnm$, $a = 881.6$, $c = 1204.4$ pm	[34]

doubled in the tungsten compound. Nonetheless, the near-neighbor environments of the two crystal structures remain quite similar. In both crystal structures the transition metal atoms have four carbo-ligands forming distorted tetrahedra. However, the Cr and W atoms are not situated in the centers of the respective tetrahedra, but in one of the triangular faces. These tetrahedra share edges and corners, thus again forming infinite three-dimensional polyanionic networks (Figs. 3 and 4).

2.2. Compounds with a metal/carbon ratio of 1.33

The next three structure types in the listing of Table 1, $Ho_2Cr_2C_3$ [2], $Er_2Mo_2C_3$ [9], and $Pr_2Mo_2C_3$ [11] with $(x+y)/z$ of 1.33 are very closely related. The crystal structure of $Ho_2Cr_2C_3$ has been determined in 1986 [2], and at this time it was assumed that the compounds $A_2Cr_2C_3$ (A = Y, Gd–Tm, Lu) and $A_2Mo_2C_3$ (A = Y, Ho–Tm, Lu) reported in that publication are all isotypic, because their monoclinic unit cells correspond to each other. Later on, when the magnetic structures of $Ho_2Mo_2C_3$ and $Er_2Mo_2C_3$ were determined by neutron diffraction [9], it was found that one of the four carbon positions in the molybdenum compounds corresponds to a position which is not occupied in $Ho_2Cr_2C_3$. On the other hand, the ordered arrangements of the rare earth and transition metal atoms in $Ho_2Cr_2C_3$ and $Er_2Mo_2C_3$ exactly correspond to each other. Recently, it was shown by careful structure determinations from single-crystal and powder X-ray diffraction data, that the new compounds $A_2Mo_2C_3$ (A = Ce, Gd, Tb, and Dy) are isotypic with $Er_2Mo_2C_3$, while $Sm_2Mo_2C_3$ adopts a $Ho_2Cr_2C_3$-type structure [8]. In the series of the nine compounds $A_2Mo_2C_3$ (A = Ce, Sm, Gd–Tm, Lu) the samarium

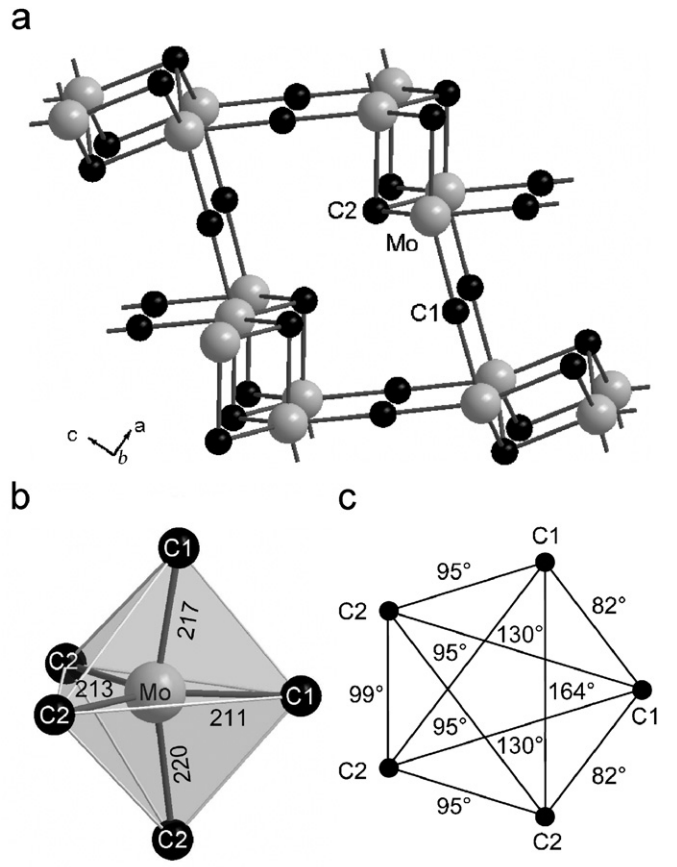

Fig. 1. Details of the crystal structure of $UMoC_2$: (a) a cutout of the polyanionic network $^{3}_{\infty}[(MoC_2)^{n-}]$; (b) carbon environment of the molybdenum atom with distances d(Mo–C) given in pm; (c) complete graph of the MoC_5 polyhedron designating the C–Mo–C angles.

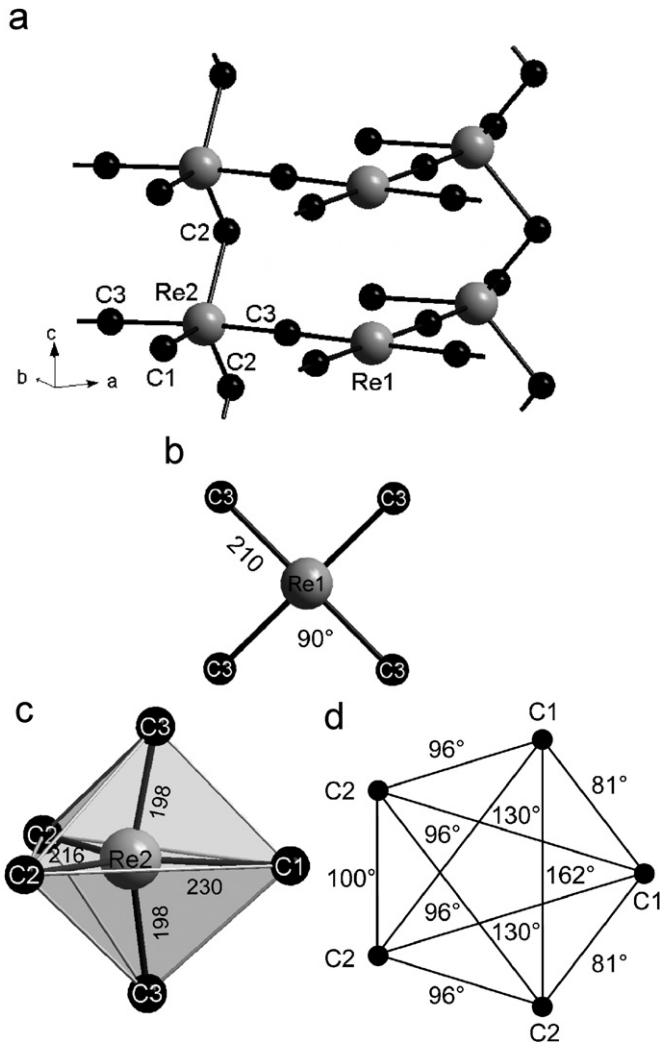

Fig. 2. Details of the crystal structure of $U_5Re_3C_8$: (a) a cutout of the polyanionic network $^{3}_{\infty}[(Re_3C_8)^{n-}]$; (b) and (c) Re(1)$C_4$ and Re(2)C_5 polyhedra with d(Re–C) given in pm; (d) complete graph of the Re(2)C_5 polyhedron with C–Re–C angles.

compound has the largest unit cell volume. The unit cell volume of the cerium compound is smaller. Apparently, here the cerium atoms are in a Ce^{IV} valence state or have mixed or intermediate $Ce^{III/IV}$ valency. Also only recently, with the even larger praseodymium atoms, a third structure type with the analogous composition $Pr_2Mo_2C_3$ has been found [11]. In these three structure types with the composition $A_2T_2C_3$ all rare earth metal atoms are coordinated by four carbon atoms. The chromium and molybdenum atoms have four carbon neighbors forming distorted tetrahedra. In the crystal structures of $Ho_2Cr_2C_3$ and $Er_2Mo_2C_3$ these TC_4 tetrahedra share edges, thus forming infinite chains which in turn are connected via common corners and in this way they form infinite polyanionic layers $^{2}_{\infty}[(T_2C_3)^{6-}]$ (T = Cr, Mo; Fig. 5). These layers are separated from each other by layers of rare earth metal atoms. In the crystal structure of $Pr_2Mo_2C_3$ four MoC_4 tetrahedra are connected by corner-sharing, thus forming tetrameric building blocks (Mo_4C_{10}). These in turn share carbon corners. But in contrast to the polyanionic layers $^{2}_{\infty}[(T_2C_3)^{6-}]$ of $Ho_2Cr_2C_3$ and $Er_2Mo_2C_3$, the building blocks (Mo_4C_{10}) in the crystal structure of $Pr_2Mo_2C_3$ form a polyanionic framework $^{3}_{\infty}[(Mo_2C_3)^{6-}]$ (Fig. 6).

2.3. Compounds with a metal/carbon ratio of 1.5

The next three entries of Table 1 reveal the same general composition A_2TC_2 with a ratio $(x+y)/z$ of 1.5. However, these three structure types—Pr_2MoC_2 [12,13], Pr_2ReC_2 [14,15], and U_2IrC_2 [16,17]—differ considerably in the dimensionality of their $[TC_2]^{n-}$ polyanions. In the crystal structure of Pr_2MoC_2 the molybdenum atoms have a distorted tetrahedral coordination by carbon. These MoC_4 tetrahedra share common edges and corners and in this way they form polyanionic layers $^{2}_{\infty}[(MoC_2)^{6-}]$ which are separated from each other by layers of Pr^{3+} ions (Fig. 7). In contrast, the rhenium atoms in Pr_2ReC_2 have only three carbo-ligands in a distorted trigonal planar arrangement. One of the two carbon positions is terminal, while the other is corner sharing with an almost linear Re–C–Re configuration, thus forming infinite polyanionic chains $^{1}_{\infty}[(ReC_2)^{6-}]$ (Fig. 8a). The third structure type is that of U_2IrC_2. Here again the valency of the uranium atoms is not known. However, this

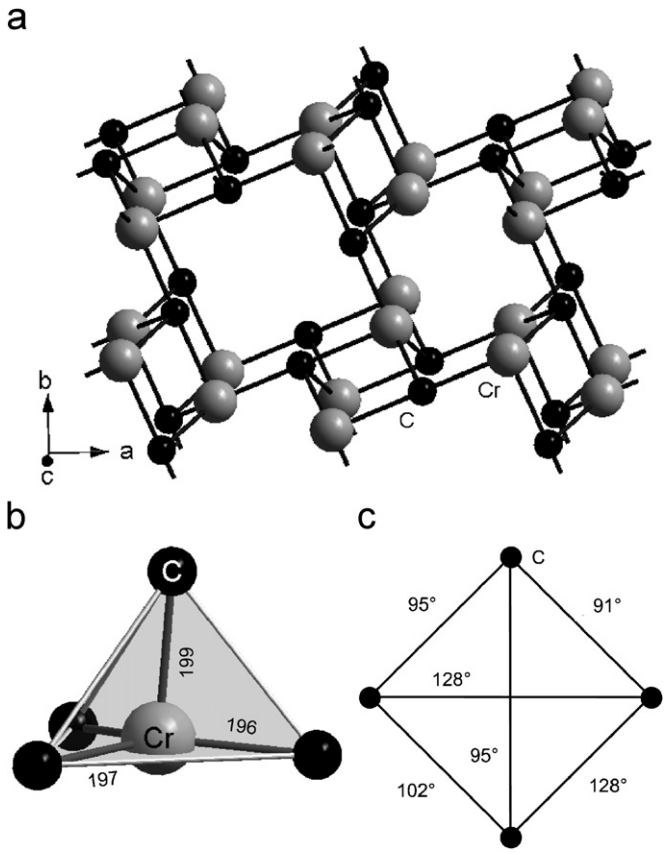

Fig. 3. Details of the crystal structure of UCr_4C_4: (a) a cutout of the polyanionic network $^{3}_{\infty}[(Cr_4C_4)^{n-}]$; (b) CrC_4 polyhedron with d(Cr–C) given in pm; (d) complete graph of the CrC_4 tetrahedron with C–Cr–C angles.

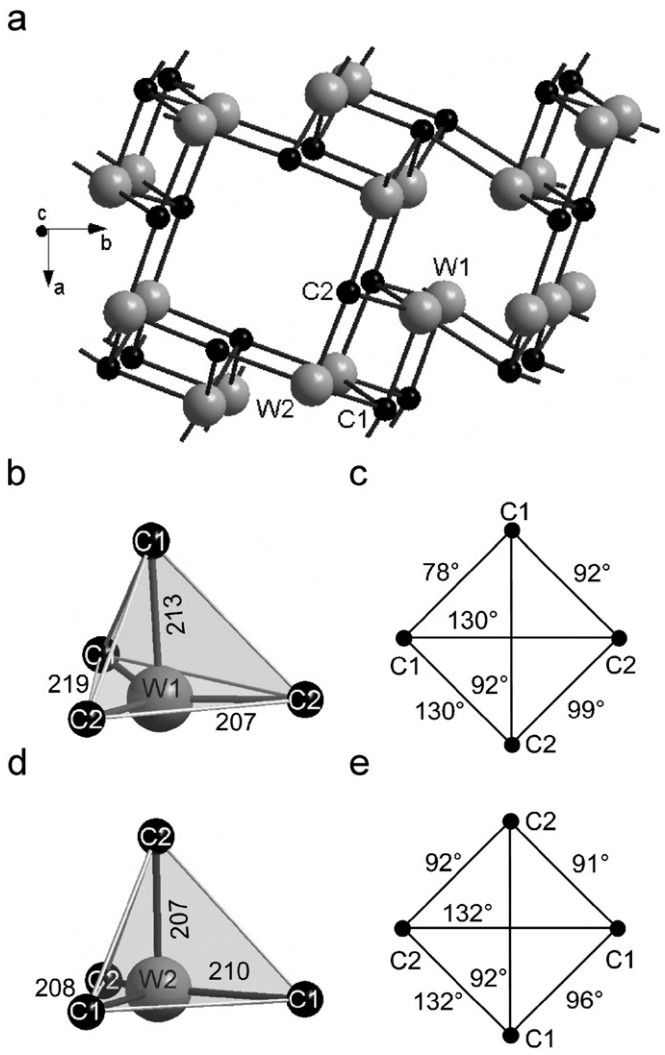

Fig. 4. Details of the crystal structure of UW_4C_4: (a) a cutout of the polyanionic network $^{3}_{\infty}[(W_4C_4)^{n-}]$; (b) and (d) WC_4 polyhedra of the two different W sites; (c) and (e) complete graphs of the WC_4 polyhedra with C–W–C angles.

crystal structure is adopted also by Th_2NiC_2, and thorium is almost always in the Th^{IV} oxidation state. Thus, the idealized formula of this compound is $Th_2^{IV}[Ni^0C_2^{-IV}]$. Here, the anionic part $[NiC_2]^{8-}$ might be regarded as zero-dimensional. It consists of linear C–Ni–C units, which are isolated from each other by the Th^{IV} species (Fig. 8b).

We note some systematic changes for the three structure types with the metal/carbon ratio of 1.5. The Pr_2MoC_2-type structure is adopted with Mo and W as the transition metal (T) components (group 6 of the periodic table). The Pr_2ReC_2-type structure occurs with the transition metals T = Re, Os (groups 7 and 8) and the U_2IrC_2-type structure is found with T = Ru, Os, Rh, Ir, Ni, Pt as transition metal components (groups 8, 9, and 10). Thus, with increasing electron counts of the T components the dimensionalities of the transition metal carbon polyanions decrease from $^{2}_{\infty}$ in Pr_2MoC_2 to $^{1}_{\infty}$ in Pr_2ReC_2 and to $^{0}_{\infty}$ in U_2IrC_2. Also, the number of carbon atoms in the first coordination shells of the transition metals decrease in the same sequence from CN = 4 in Pr_2MoC_2 to CN = 3 in Pr_2ReC_2 and to CN = 2 in U_2IrC_2.

2.4. Compounds with a metal/carbon ratio of 2

The two compounds YCoC [18] and $La_5Os_3C_{4-x}$ [20] have the common metal to carbon ratio $(x+y)/z$ of 2. Of these, YCoC may be considered as a pure carbometalate, while the other compound contains one carbon position with considerable defects. The crystal structure of YCoC is extremely simple. It is tetragonal with only one crystallographic site for each atomic species. The metal atoms occupy the positions of two CsCl cells on top of each other. Each carbon atom is situated between two cobalt atoms. In this way linear polyanionic chains $^{1}_{\infty}[(Co^{I}C^{-IV})^{3-}]$ are formed (Fig. 8c) which alternate along [0 0 1] and extend parallel to the x and y axes of the tetragonal unit cell.

The compound $La_5Os_3C_{4-x}$ contains structural characteristics of both the carbometalates and the interstitial carbides and may therefore be classified as a carbometalate-carbide. One carbon position shows octahedral La coordination and no transition metal neighbors. This position was found to be occupied to only 25(4)% [20]. The other carbon position has two osmium neighbors in a slightly bent arrangement within an infinite zig-zag

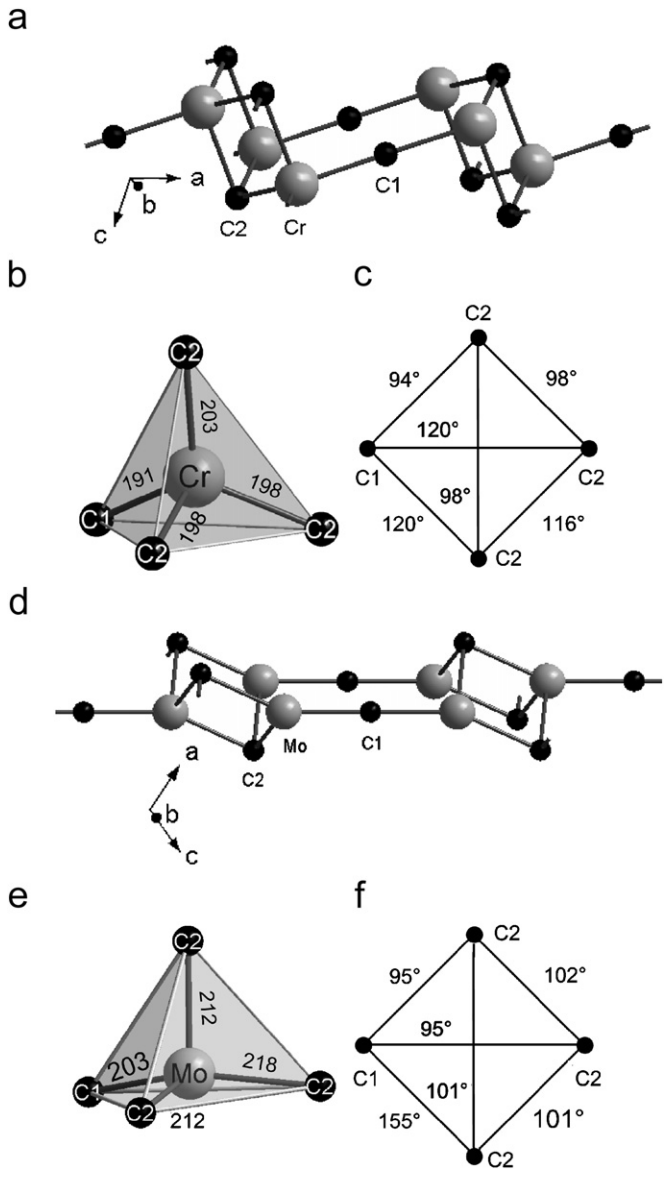

Fig. 5. Details of the crystal structures of $Ho_2Cr_2C_3$ and $Er_2Mo_2C_3$: (a) cutouts from the polyanionic layers (a) $^2_\infty[(Cr_2C_3)^{6-}]$ and b) $^2_\infty[(Mo_2C_3)^{6-}]$; (c) and (e) corresponding TC_4 (T = Cr, Mo) polyhedra; (d) and (f) complete graphs of TC_4 polyhedra.

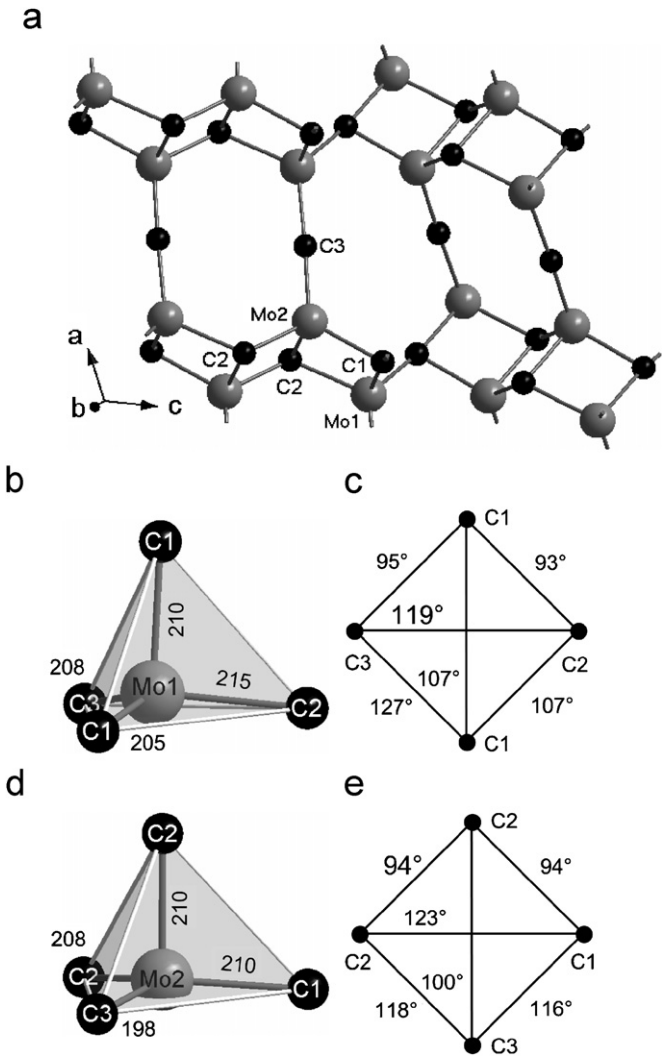

Fig. 6. Details of the crystal structure of $Pr_2Mo_2C_3$: (a) a cutout of the polyanionic network $^3_\infty[(Mo_2C_3)^{6-}]$; (b) and (d) MoC_4 polyhedra of the two crystallographic different Mo sites with d(Mo–C) given in pm; (c) and (e) complete graphs of MoC_4 polyhedra with C–Mo–C angles.

chain (Fig. 8d). Using oxidation numbers and charges the compound may be written with the formula $(La^{III})_5[Os_3C_3]^{14-}(0.25C^{4-})^{1-}$. Since there is only one crystallographic osmium site, this results in a fractional oxidation number for the osmium atom.

2.5. Compounds with metal/carbon ratios $\geqslant 4$

The remaining compounds of Table 1 have considerably higher metal to carbon ratios than the compounds just discussed. The carbon atoms in these remaining compounds $A_xT_yC_z$ usually occupy octahedral positions formed and surrounded by both the A and T atoms. Frequently these carbon positions are not fully occupied. For instance, the structure refinements of the carbides $LaMn_{11}C_{2-x}$ [23], $Pr_2Mn_{17}C_{3-x}$ [25], and $Tb_2Mn_{17}C_{3-x}$ [26] from single-crystal X-ray diffraction data resulted in occupancy values of 76(1)%, 59(3)%, and 81(4)%, respectively. It can be expected that due to the partial occupancy of the carbon sites there are substantial homogeneity ranges, however, these have not been explored up to now. With respect to the fractional occupancy of the carbon positions these ternary carbides resemble the well-known binary transition metal carbides e.g. TiC_{1-x}, VC_{1-x}, etc. which are frequently called "interstitial carbides". For that reason we sometimes designate this name also to the ternary compounds $A_xT_yC_z$ with metal/carbon ratios $(x+y)/z \geqslant 4$. For many structure types of these ternary carbides with a high metal content, the binary "unfilled" structure types are also known. Thus, for instance, in the perovskite carbide $ThRu_3C$ the Th and Ru atoms occupy the positions of the Au and Cu atoms, respectively, of the well-known cubic Cu_3Au-type

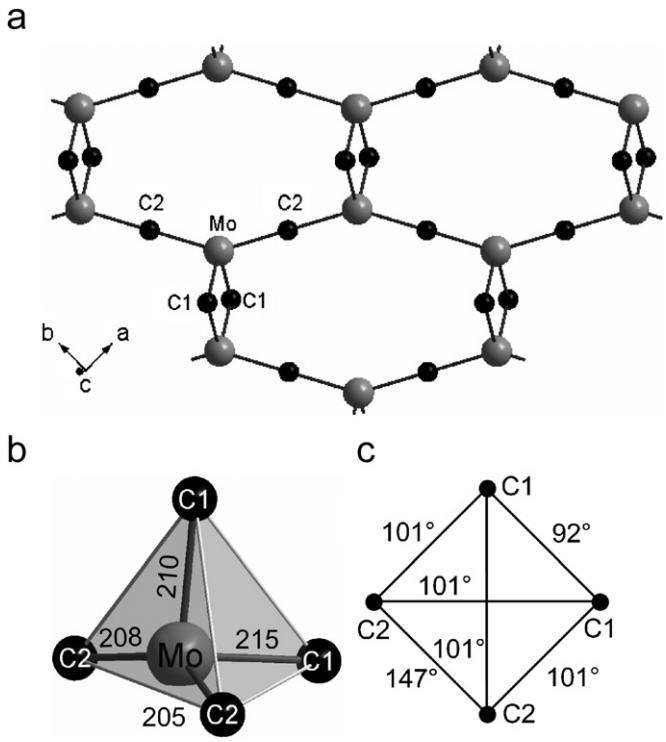

Fig. 7. Details of the crystal structure of Pr_2MoC_2: (a) a cutout of the polyanionic layer $^2_\infty[(MoC_2)^{6-}]$; (b) MoC_4 polyhedron with d(Mo–C) given in pm; (d) complete graph of the MoC_4 tetrahedron with C–Mo–C angles.

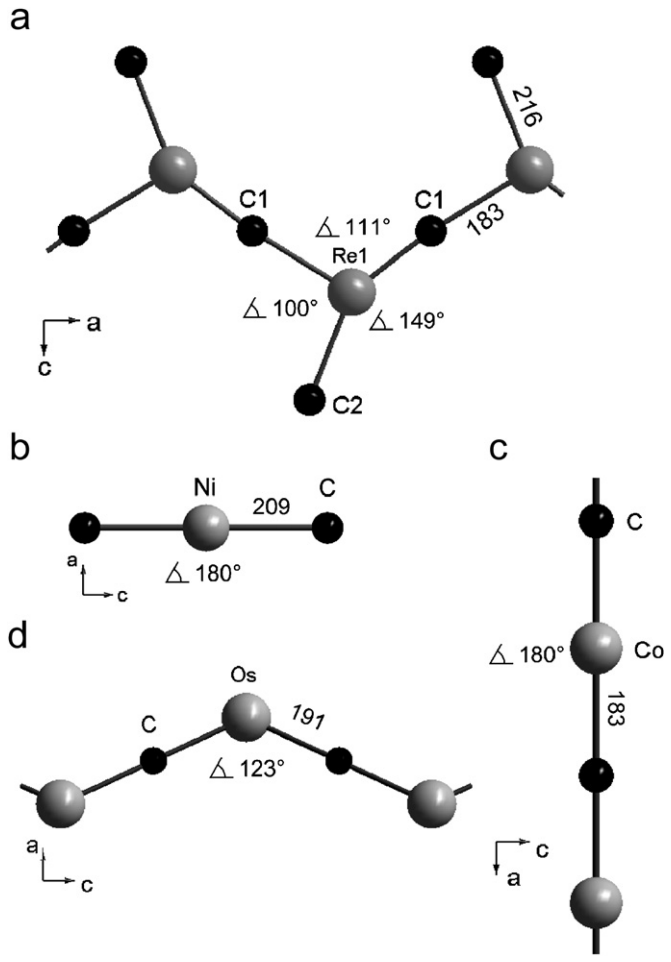

Fig. 8. Polyanions of selected compounds: (a) $^1_\infty[(ReC_2)^{6-}]$ zigzag chain in Pr_2ReC_2, (b) discrete complex anion $[NiC_2]^{8-}$ in the crystal structure of Th_2NiC_2, (c) $^1_\infty[(CoC)^{3-}]$ linear chain in the crystal structure of YCoC; (d) $^1_\infty$[OsC] zigzag chain in the crystal structure of $La_5Os_3C_{4-x}$.

structure. Other examples include the ternary compounds $LaMn_{11}C_{2-x}$, $Pr_2Mn_{17}C_{3-x}$, and $Tb_2Mn_{17}C_{3-x}$, where the positions of the metal atoms exactly correspond to those of the binary intermetallics $BaCd_{11}$ [40], Th_2Zn_{17} [41], and Th_2Ni_{17} [42]. Thus, the ternary interstitial carbides and the binary "host" structures also have the same space group symmetry. In these ternary compounds the total electron count for the metal atoms is usually smaller for ternary carbides than for the binary host structures [14]. In the present paper, we focus on the carbides with a low metal/carbon ratio—the carbometalates—and we will not further discuss the structural chemistry of the metal-rich interstitial carbides.

3. Chemical bonding in carbometalates and metal-rich carbides

In the third column of Table 1 we have assigned oxidation numbers to the metal and carbon atoms of the ternary compounds $A_xT_yC_z$ in agreement with their classification as carbometalates. For some of these compounds chemical bonding has already been examined in the literature on the basis of the observed interatomic distances. As will be discussed in more detail below, these compounds owe their stability not only to metal–carbon interactions. They also have relatively short metal–metal distances, indicating significant metal–metal bonding. Generally, three kinds of metal–metal bonding (M–M) can be distinguished: A–A, A–T, and T–T bonding. Of these three, only the A–A bonding affects the total electron count of the $[TC]^{n-}$ polyanion, since A–A bonding can be achieved only if the A valence states are populated at least to some extent. In this case the charge transfer from the A species to the anionic structural part is smaller than indicated by the assignment of the respective oxidation numbers. For that reason the formulae in the third column of Table 1 have to be considered as idealized, aiming for integer oxidation numbers. This is justified, since the deviations from the ideal values are small, as it will be discussed below.

For some of the carbometalates listed in Table 1 it was attempted to rationalize chemical bonding on the basis of the observed interatomic distances using the Lewis formalism to show bonding electrons and aiming for an electron count of 8 for the carbon atoms (C^{4-} species) and sometimes also for a count of 18 for the transition metal atoms. Inherently, this formalism is not well suited for band structures, since a fractional occupancy of electrons per atom cannot be represented. On the other hand, no

computers are needed to show a picture of the approximate electron distribution. Such Lewis formulae have been published for Er_2ReC_2 [14], Th_2NiC_2 [17], $La_5Os_3C_{3.25}$ [20], $Ho_2Cr_2C_3$ [9], and $Er_2Mo_2C_3$ [9]. R.B. King considered the transition metal–carbon polyanions $[TC]^{n-}$ as organometallic polymers and arrived at electron counts between 14 and 18 for the transition metal atoms in the compounds YCoC, Y_2ReC_2, Th_2NiC_2 [43,44], $Ho_2Cr_2C_3$, and $Er_2Mo_2C_3$ [45]. Extended Hückel tight binding (EHT) calculations have been carried out for the polyanionic chains $^1_\infty[(CoC)^{3-}]$ in YCoC and $^1_\infty[(ReC_2)^{6-}]$ in Er_2ReC_2 by Hoffmann and coworkers [46,47]. In their calculations for Er_2ReC_2 significant Re–C antibonding contributions are found at and below E_F. In our calculations reported below these contributions are much decreased due to minor orbital contributions of carbon atoms in the upper part of the band structure. As a source of this discrepancy the EHT parameters used for the calculations are the weak point: the ionization energies used for the Re(4*d*) orbitals place them below C(2*p*) making them the electron acceptors with respect to carbon *p* orbitals. Furthermore, the Re–C antibonding states are mainly composed of C states, while in our DFT calculations they are Re majority states and carbon has only minor contributions in the upper part of the band structure, which makes the Re–C antibonding contributions of minor importance. Noteworthy, on the basis of the EHT calculations the existence of an electron-poorer compound has been predicted, while the isostructural electron-richer Os compound has been found later instead. In addition, EHT calculations have also been used for a study of chemical bonding of $Ho_2Cr_2C_3$ and related carbides by Koo and Whangbo [48]. According to them, the bonding within the discrete linear chain units Cr–C–Cr should be considered as double bonds. A striking difference to our calculations (see below) is obtained for the Cr–Cr interaction which has a strong antibonding peak of COOP being occupied, whereas in our calculations significant antibonding states are not occupied. Since the orbital energy parameters used for Cr(3*d*) are higher than for C(2*p*) in their calculations, which is consistent with our findings, possibly the neglect of the rare earth environment is responsible for this discrepancy.

3.1. Theory

In our present study scalar-relativistic band structures were calculated for representative rare earth metal carbometalates and the metal-rich carbide YRh_3C (see Table 3) using the LMTO-ASA method [49] in the local density approximation (LDA). Since the LDA-approximation results in too itinerant *f*-electrons, the yttrium compounds have been chosen as representatives. However, for two structure types, $Pr_2Mo_2C_3$ and Pr_2MoC_2, hypothetical lanthanum compounds have been treated since no yttrium compounds are obtained so far. Crystallographic data were taken from the literature (see Table 1 and 2). The radii of the atomic and empty spheres (ES) were determined according to the standard procedure as described in [50]. The partial waves of Y(5*s*, 4*d*), La(6*s*, 5*d*, 4*f*), Cr(4*s*, 4*p*, 3*d*), Co(4*s*, 4*p*, 3*d*), Mo(5*s*, 5*p*, 4*d*), Rh(5*s*, 5*p*, 4*d*), Re(6*s*, 6*p*, 5*d*), Os(6*s*, 6*p*, 5*d*), and C(2*s*, 2*p*) were explicitly included in the Hamiltonian, while those of Y(5*p*, 4*f*), La(6*p*), Mo(4*f*), Rh(4*f*), Re(5*f*), Os (5*f*), C(3*d*) and ES(all orbitals) were treated according to the Löwdin downfolding technique [51]. Chemical bonding properties were investigated by analyzing the crystal orbital Hamilton population (COHP) [52].

3.2. Chemical bonding in carbometalates

In our former studies of the electronic structure of rare earth metal carbometalates Pr_2MoC_2 [12] and $Pr_2Mo_2C_3$ [11] it has been worked out exemplarily that covalent bonding of each *T*–C bond is stronger compared with each bond *A*–C. This forms the basis for separating the complex carbometalate anion from the rare earth metal partial structure. Furthermore, although interactions *A*–C reveal a significant covalent character, the oxidation states of the rare earth species have to be considered as III since no *A* majority band states are occupied below the Fermi level. Nevertheless, covalent interactions *A*–*A* can be detected, but their occurrence is due to partial covalent bonding *A*–C, which results in partially occupied rare earth orbitals. This observation is consistent with the assigned oxidation states. The assignment of oxidation states within the carbometalate anion is done on the basis of atomic electronegativities giving −IV for the carbon species and an overall compensating oxidation state for *T*. The strongly covalent interactions *T*–C and the fact that both species naturally have occupied majority bands make an assignment of oxidations states for *T* and C species on the basis of the band structure somewhat problematic.

In the present investigation the overview (Table 3) of the electronic structures is restricted to the rare earth carbometalates and excludes the actinoid compounds. The following discussion is based on LMTO-ASA calculations using the COHP method, not only by comparing each individual bond but also by including the respective bond multiplicities per formula unit, such that the orbital interaction part of the band structure energy per formula unit is monitored. The bond multiplicities have not explicitly been included in all the earlier discussions [11,12]. While for interactions *T*–C and *A*–C the distance d_{max}—above which interactions are neglected due to their smallness—is obvious from the crystal structure, this is not the case for metal–metal interactions due to their longer range. The corresponding values of distances are indicated in Table 3. In total, there are five different types of interactions to be considered, namely *T*–C, *A*–C, *T*–*T*, *A*–*T*, and *A*–*A*. Thus, for each representative compound treated here two kinds of COHP(*E*) diagrams are shown in Fig. 9: (i) bond interactions averaged over all crystallographic different species corresponding to the five different interactions and (ii) those bond interactions

Table 3
Integrated crystal orbital Hamiltonian populations (–ICOHP) for near-neighbor interactions M–M and M–C ($M = A$, T) within the given distance ranges in pm for selected carbometalates and the metal-rich carbide YRh_3C; the next occurring distances d_{max}, outside the ranges are given in parentheses; –ICOHP are listed as averaged values and also as weighted by the respective bond frequencies per formula unit

Type	N	Distance range	Average	Weighted
$Y_2Cr_2C_3$[a]				
Cr–C	8 ×	191–204 (387)	4.77	38.16
Y–C	10 ×	242–264 (329)	1.35	13.50
Y–Cr	10 ×	300–316 (349)	0.47	4.70
Y–Y	6 ×	339–342 (479)	0.16	0.96
Cr–Cr	2 ×	265 (337)	1.08	2.16
$COHP_{M-M} : COHP_{M-C} = 1 : 6.6$				
$La_2Mo_2C_3$[c]				
Mo–C	8 ×	198–215 (375)	4.01	32.08
La–C	10 ×	255–289 (353)	1.21	12.10
La–Mo	15 ×	323–370 (463)	0.39	5.85
La–La	4.5 ×	329–364 (382)	0.22	0.99
Mo–Mo	1.5 ×	286–288 (313)	0.78	1.17
$COHP_{M-M} : COHP_{M-C} = 1 : 5.5$				
La_2MoC_2[c]				
Mo–C	4 ×	209–214 (406)	3.86	15.44
La–C	8 ×	249–265 (398)	1.54	12.32
La–Mo	10 ×	330–356 (469)	0.39	3.90
La–La	6 ×	322–355 (420)	0.29	1.74
Mo–Mo	0.5 ×	290 (429)	0.75	0.38
$COHP_{M-M} : COHP_{M-C} = 1 : 4.6$				
Y_2OsC_2[b]				
Os–C	3 ×	187–197 (402)	5.72	17.16
Y–C	9 ×	244–269 (406)	1.27	11.43
Y–Os	8 ×	307–333 (357)	0.49	3.92
Y–Y	8 ×	329–367 (488)	0.24	1.93
Os–Os	—	— (392)	—	—
$COHP_{M-M} : COHP_{M-C} = 1 : 4.9$				
Y_2ReC_2[b]				
Re–C	3 ×	195–205 (401)	5.42	16.26
Y–C	9 ×	249–265 (411)	1.43	12.87
Y–Re	8 ×	308–337 (363)	0.61	4.88
Y–Y	8 ×	334–366 (501)	0.22	1.76
Re–Re	—	— (403)	—	—
$COHP_{M-M} : COHP_{M-C} = 1 : 4.4$				
YCoC				
Co–C	2 ×	183 (389)	5.44	10.88
Y–C	4 ×	251 (443)	1.57	6.28
Y–Co	8 ×	310 (576)	0.56	4.48
Y–Y	3 ×	343–365 (501)	0.22	0.66
Co–Co	1 ×	343 (365)	0.16	0.16
$COHP_{M-M} : COHP_{M-C} = 1 : 3.2$				
YRh_3C				
Rh–C	6 ×	207 (462)	3.58	21.48
Y–C	—	− (358)	—	
Y–Rh	12 ×	292 (506)	1.08	12.96
Y–Y	—	− (413)	—	—
Rh–Rh	12 ×	292 (413)	0.50	6.00
$COHP_{M-M} : COHP_{M-C} = 1 : 1.1$				

[a]Lattice parameters taken from powder XRD of $Y_2Cr_2C_3$ and atomic coordinates from single crystal XRD of $Ho_2Cr_2C_3$.
[b]Lattice parameters taken from powder XRD of Y_2ReC_2 and Y_2OsC_2 and atomic coordinates from single crystal XRD of Er_2ReC_2 and Tb_2OsC_2, respectively.
[c]Hypothetical compounds with crystal structure data taken from the corresponding Pr compounds.

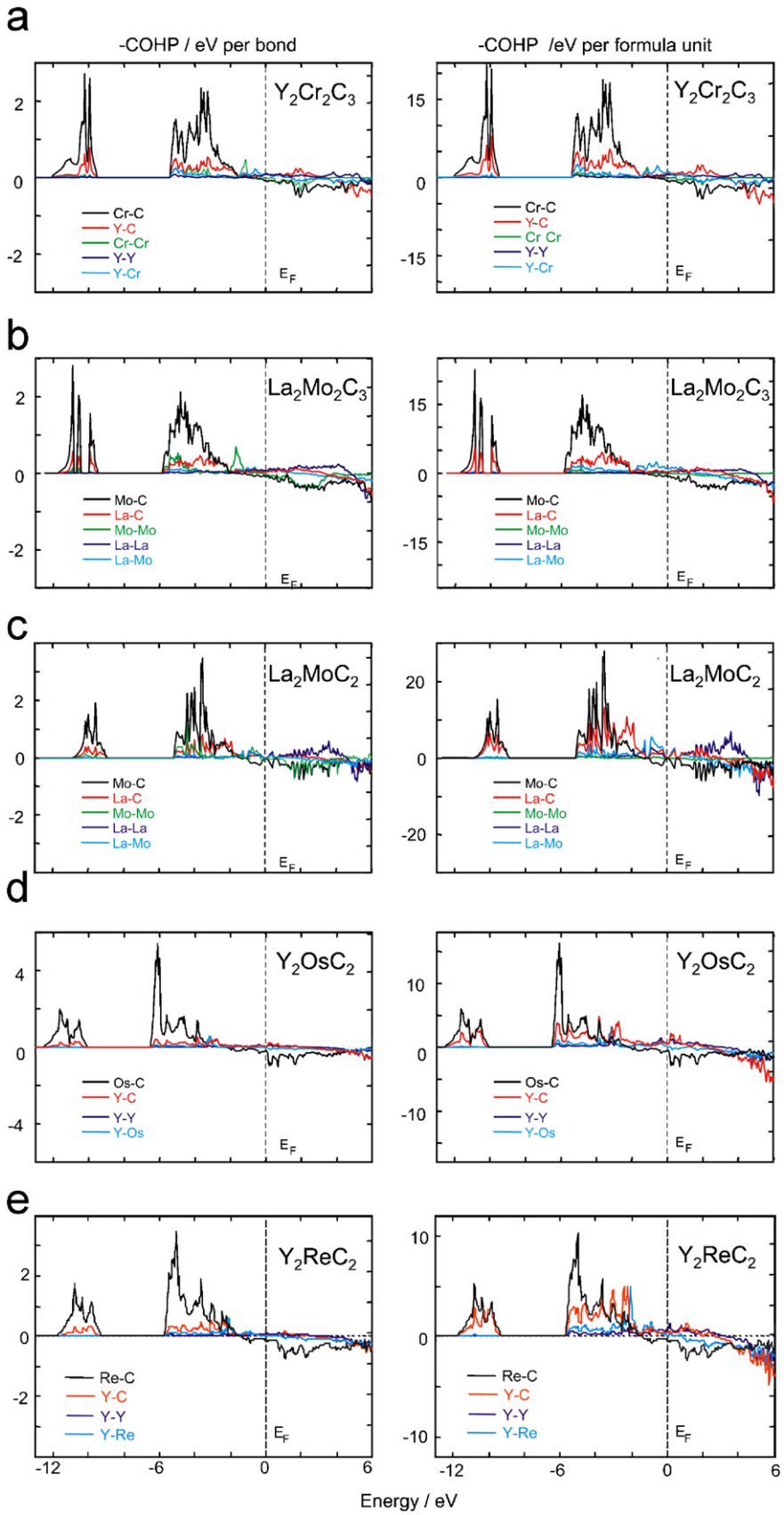

Fig. 9. Crystal orbital Hamilton population curves for the various *M*–C and *M*–*M* interactions of selected carbometalates; averaged interactions and those weighted by the respective bond frequencies per formula unit are shown on the left and right hand sides, respectively: (a) $Y_2Cr_2C_3$; (b) $La_2Mo_2C_3$; (c) La_2MoC_2; (d) Y_2OsC_2; (e) Y_2ReC_2; YCoC.

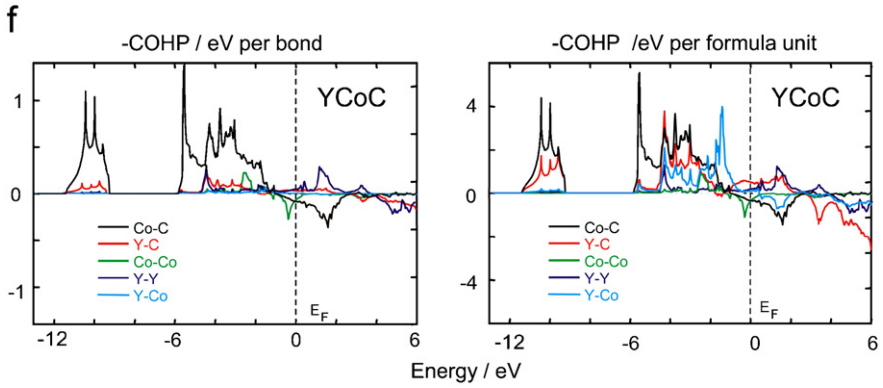

Fig. 9. (*Continued*)

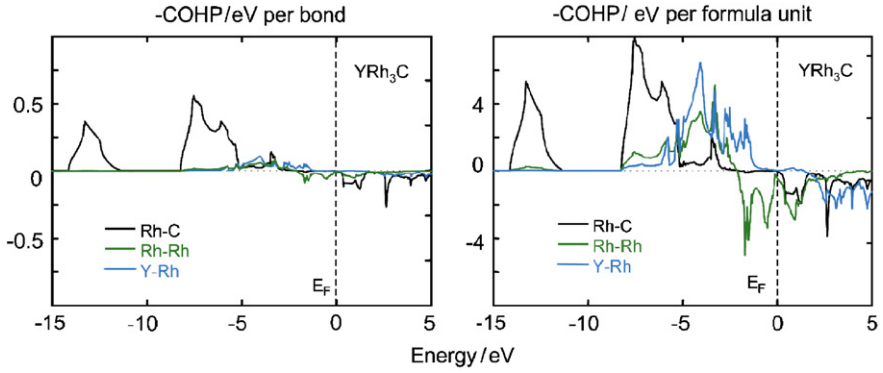

Fig. 10. Crystal orbital Hamilton population curves for Rh–C, Rh–Rh, and Y–Rh interactions in YRh_3C; individual interactions and those weighted by the respective bond frequencies per formula unit are shown on the left and right hand side, respectively. The calculations were carried out for the ideal composition YRh_3C. The real composition may have carbon defects: YRh_3C_{1-x}, as is frequently observed for interstitial carbides [22].

weighted by the respective bond multiplicities per formula unit. Thus, while the averaged diagrams—in a sense—give information about the local importance of a covalent interaction type, the COHP diagrams weighted by bond multiplicities contain information about the relative importance of certain kinds of interaction for the whole crystal structure.

A number of findings can be given for all carbometalate compounds considered hereafter and exactly right these characterize the chemical bonding of a rare earth metal carbometalate. These criteria will be used to distinguish the rare earth metal carbometalates from the metal-rich interstitial carbides (see Figs. 9 and 10 and Table 3).

For each carbon species the bonds between the carbon atoms and the transition metal (T–C) are pronouncedly more covalent as the interactions A–C. Although, in all cases the number of covalent bonds A–C is larger than the number of bonds T–C the latter are still dominating in sum (compare weighted COHP(T–C) vs. COHP(A–C)). COHP diagrams for T–C interactions always exhibit occupancies of weakly antibonding bands in the upper part of the band structure but the strongly antibonding bands are always placed above E_F. In contrast, the COHP diagrams for A–C interactions always display a non-exhausted covalent bonding interaction with a significant number of bonding states being left unoccupied, which is consistent with the attributed oxidation states.

The upper part of the band structures (already below E_F) is dominated by metal–metal interactions which are generally weaker than the metal–carbon interactions, both in comparison one-by-one and also in total. Among the metal–metal interactions there is a sequence of decreasing covalent bonding strength according to T–T > A–T > A–A in those cases where all three kinds of interactions occur. Noteworthy, strongly antibonding T–T interactions are avoided for the more electron rich T species in Y_2ReC_2, Y_2OsC_2 (Fig. 9d,e) and YCoC (Fig. 9f) for which large distances T–T are observed. Those are even weaker in covalent bond strength than the A–A interactions. In total, for all carbometalates the donor acceptor bonds A–T are more important than the T–T interactions due to their higher frequency. For those carbometalates with T having formally less than 5 remaining electrons the covalent bonding interactions are seen not to get fully exhausted at E_F (Fig. 9a–c). In those cases, where the electron richness of T leads to avoidance of strong T–T interactions, covalent bonding interactions A–T gain in strength. They are seen to get exhausted approximately at E_F, with all antibonding interactions being left unoccupied (Fig. 9d–f). The weakest metal–metal interactions occur between rare

earth species (A–A) and they always display available bonding interactions above E_F. Partial covalency A–C is the cause for significant residual electronic population of A, which also leads to minor A–A bonding interactions, an observation which is consistent in general with the picture of an interaction between formally naked cations.

Summing up, the carbometalate anions may be regarded as structural entities, which contain the T–C bonds as the strongest covalent interactions in these compounds. T–T bonding within the complex anion is found in special cases, where the electron count on T is not too high, i.e., where T has formally less than five (remaining) electrons. The covalent interaction between the complex anion and the surrounding rare earth metal species is provided by A–C and A–T bondings, the more important being the former one.

3.3. Chemical bonding in the metal-rich carbide YRh_3C

According to Table 1 the YRh_3C-type compounds with a $(x+y)/z$ ratio of 4 are those metal-rich carbides which are closest to carbometalates. Therefore, the electronic structure of YRh_3C will be compared on the basis of COHP diagrams (Fig. 10) with those of the carbometalates discussed above (Fig. 9). Bonding interactions Rh–C are strongly covalent and are fully exhausted below E_F without antibonding contributions being occupied. In fact, in the crystal structure of YRh_3C the Y–C interactions are even shielded by Rh atoms which enclose all C atoms.

Concerning individual metal–metal interactions, the Rh–Rh orbital interactions are sizable, but a large amount of antibonding Rh–Rh bands is occupied as well, which reduces the overall covalent Rh–Rh bonding by about 40%. The real structure may have some carbon-defects, as is frequently observed for interstitial carbides [22]. This would not greatly affect the band structure, except that the Fermi level would be somewhat lower, thus leaving the antibonding Rh–Rh bands less occupied. For compensation the mixed metal orbital interactions Y–Rh play an important role since they are comparably strong and bonding combinations are fully exhausted up to E_F. It would be interesting to analyse interactions Y–Y as compared to those in carbometalates described above. This is however not possible under comparable conditions, since the distance Y–Y of 412 pm is too large to give rise to sizable interactions although Y is expected to be significantly electron richer compared with the respective situation in carbometalates.

Comparing carbometalates and YRh_3C on the basis of individual bonds there is not much of a difference. Unfortunately the interactions, A–A and A–C, which should be enhanced due to a significantly larger electronic population of the A species, are disfavoured by the crystal structure. The major difference to carbometalates is seen considering the bond multiplicities weigthed COHP diagrams (Fig. 10) and the ratios $COHP_{M-M}/COHP_{M-C}$ (Table 3). The relative importance of metal–metal bonds with respect to metal carbon bonds has strongly increased from values of maximally 1/3 (YCoC) to 1/1 in YRh_3C (Table 3). It is very interesting to note the different behavior with respect to the strongly antibonding T–T contributions. While in the carbometalates the complex anion adopts a structure where these few T–T interactions are decreased in total, in the metal-rich carbide YRh_3C these numerous interactions are counterbalanced by the mixed metal interactions A–T and no structural relaxation occurs at all. Thus, the anionic part of the carbometalate sensibly reacts on unfavourable individual interactions within its framework, while the carbide YRh_3C reacts as an entity where the sum of collective interactions counterbalances less favourable individual ones.

4. Carbometalates compared to nitridometalates as well as to oxo- and fluorometalates

Nitridometalates represent a well established class of compounds containing complex anions $[T_xN_y]^{n-}$ which are balanced in charge by cationic components from the first and the second group of the periodic table (alkali and alkaline-earth metal elements). It became already clear in 1997 [53] that one of the most interesting chemical aspects of the nitridometalates is the preferred stabilisation of low oxidation states of the transition metal elements, especially of those with group-numbers $\geqslant 7$. In fact, this means that nitridonickelates(I), -cobaltates(I), -ferrates(I), and manganates(I) are not exceptional [54–56], and even lower valence states can be realized as was already shown by $Ba_2[Ni_3N_2]$ with an average oxidation state for Ni of $+2/3$ [57].

The general idea is that the higher polarizabilty of the nitrido-ligand compared to the respective oxo-ligand causes the stabilization of lower oxidation states of the transition metal elements which are involved in the formation of the complex anions. In other words, the sequence of monoatomic ligands "$F^- \rightarrow O^{2-} \rightarrow N^{3-}$" representing increasing polarizibility could be extended to the carbo-ligand C^{4-}, thereby opening the chance for stabilization of even lower oxidation states of the transition metal elements participating in the formation of complex carbometalate units $[T_xC_y]^{n-}$.

By this, it becomes clear that the charge of the complex carbometalate anions will significantly increase compared to the nitride complexes and for reasons of charge compensation electropositive components are needed with a cationic charge as high as possible. This may be one of the reasons why the carbometalates known up to now (see Table 1) exclusively contain rare earth metals and actinoids with their common valence states A^{III} and A^{IV}. Alkali and alkaline-earth compounds do not form with monoatomic C^{4-} species. Instead these low-valency metals form compounds, where the carbon atoms have lower oxidation states, i.e. acetylides and allylenides [58,59].

As nature is dominated by continuity and abrupt changes are mostly avoided closer relationships between

the complex anions in nitrido- and carbometalates can be expected and are actually obvious as will be demonstrated exemplarily for the polyanionic structures shown in Fig. 8 (see also Table 1). $Th_2^{IV}[Ni^0C_2]$ [17] contains linear dumbbell ions $[CNi^0C]^{8-}$ which are isostructural to the $[NFe^{II}N]^{4-}$ units in the respective lithium compound [60]. $Y[Co^IC]$ [18] contains infinite linear chains $^1_\infty[(Co^IC_{2/2})^{3-}]$, a structural motif which is also present in the isotypic crystal structure of $Ca[Ni^IN]$ [61,62]. The crystal structure of $Pr_2[Re^{II}C_2]$ [15] contains polyanions $^1_\infty[(Re^{II}C_{2/2}C)^{6-}]$ with Re^{II} in a distorted trigonal-planar coordination by the carbo-ligands. Trigonal-planar coordination of transition metal elements with various distortions (from ideal to T-shaped) and with various dimensionalities of the complex anions are also observed in the crystal structures of nitridoferrates(III) and –(II) [53]. Further examples for the close structural relationships between nitrido- and carbometalates could be added but shall be restricted here to the comparison of general trends in the respective Mo compounds only.

Whereas tetrahedral coordination of Mo is observed in nitrido- as well as in carbomolybdates essential differences are present in the oxidation states of the transition metal element. The highest oxidation state of Mo in carbomolybdates with tetrahedral anionic structures is III whereas in tetrahedral nitridomolybdates the highest possible oxidation state (VI) is easily reached (e.g., $Li_6[Mo^{VI}N_4]$ [69] and $Ba_3[Mo^{VI}N_4]$ [179]). Although, the specifically directed research in the preparation and characterization of carbometalates is rather young [12] and the number of known representatives is therefore clearly limited, it seems to be already of general chemical interest to compare the trends in oxidation states of the transition metal elements by taking into account not only the carbo- and nitridometalates but also the respective oxo- and fluorocompounds. At the moment this investigation has to be restricted to compounds containing transition metals from groups 5 to 10 because up to now examples of carbometalates are known only from this part of the periodic table.

In Fig. 12 the maximum oxidation states of the transition metals elements in carbo-, nitrido-, oxo-, and fluorometalates are shown without distinguishing between 3*d*, 4*d*, and 5*d* elements. This distinction is accounted for in Fig. 11 (see Table 4) where not only the highest oxidation states of the transition metal elements of the groups 5–10 are listed, but all oxidation states which are known from the literature. The highest oxidation states of the transition metal elements are realized in the oxo-compounds because in spite of their greater electronegativity the fluoro-ligands carry only one negative charge. Thus, for instance, in the well-known oxide RuO_4 the Ru atoms with tetrahedral oxygen coordination are in the oxidation state VIII, whereas in a corresponding hypothetical compound RuF_8 the 8 fluorine ions can not sufficiently approach the small Ru atom for steric reasons. For group 5 elements the maximum oxidation state is reached in all the metalates under consideration, the same is true for groups 6 and 7

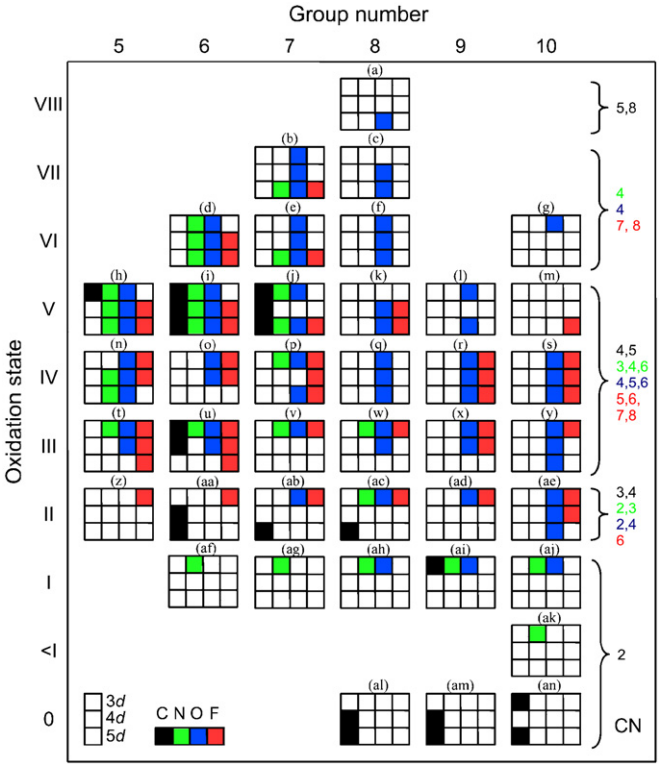

Fig. 11. Oxidation states and coordination numbers of 3*d*, 4*d*, 5*d* -metals in carbo-, nitrido-, oxo-, and fluorometalates. Labels correspond to those used in Table 4.

except for the carbometalates which only reach the oxidation state V for the transition metal elements. The graded slopes in Fig. 12 starting from group 7 and 8, respectively, clearly follow the trend of decreasing oxidation states of the transition metal elements with the sequence oxo-, nitrido-, carbometalates.

By careful discussion of the trends shown in Fig. 12 one should be aware that the given values are regarded as representative for normal pressure conditions. It can be expected that by increasing the reaction pressure even higher oxidation states may be reached for the transition metal elements with the higher group numbers. First indications in that direction were already obtained for the nitridometalates of groups 9 and 10. Finally, with regard to Table 4 we point out, that the lowest valence states (0) for transition metal elements of groups 8–10 are reached in the carbometalates.

5. Conclusion

We have classified ternary carbides $A_xT_yC_z$ (A = rare earth metals and actinoids; T = transition metals) with monoatomic species C^{4-} as structural entities on the basis of the metal to carbon ratios $(x+y)/z$. Two main groups can be distinguished: carbometalates and metal-rich carbides. And this distinction is justified by a number of findings: (i) carbometalates form with a defined chemical composition without significant

Table 4
Oxidation states of 3*d*, 4*d*, 5*d* -metals in carbo-, nitrido-, oxo-, and fluorometalates; for each oxidation state one example and the reference is given. Labels correspond to those used in Fig. 11

Label	Carbon	Nitrogen	Oxygen	Fluorine
(a)	—	—	$K_2Os^{VIII}O_5$ [63]	—
(b)	—	$Li_5Re^{VII}N_4$ [64]	$KM^{VII}O_4$, M = Mn,Tc,Re [65]	$CsRe^{VII}F_8$ [66]
(c)			$KM^{VII}O_4$, M = Ru,Os [67,68]	
(d)		$Li_6M^{VI}N_4$ M = Cr,Mo,W [69]	$K_2M^{VI}O_4$, M = Cr,Mo,W [65]	$CsM^{VI}F_7$, M = Mo,W [70]
(e)		$(Li_2Ca_4O)_3(Re^{VI}N_4)_4$ [71]	$K_2M^{VI}O_4$, M = Mn,Tc,Re [65]	$K_2Re^{VI}F_8$ [72]
(f)			$K_2Fe^{VI}O_4$, $Na_2Ru^{VI}O_4$, $Ba_2Os^{VI}O_5$ [73–75]	
(g)			$K_2Ni^{VI}O_4$ [76]	
(h)	$U^{III/IV}V^{V/IV}C_2$[a] [2]	$Li_7M^{V}N_4$, M = V,Nb,Ta [77–79]	$NaV^{V}O_3$, $YM^{V}O_4$, M = Nb,Ta [80–82]	$K_2M^{V}F_7$, M = Nb/Ta [83,84]
(i)	$U^{III/IV}Cr^{V/IV}C_2$,[a] $YM^{V}C_2$, M = Mo,W [2]	$Ba_5Cr^{V}N_5$, $LiMo^{V}N_2$, $Li_{0.84}W^{V}_{1.16}N_2$ [85–87]	$NdCr^{V}O_4$, $La_5Mo_6^{IV/V}O_{21}$, $Na_{0.74}W^{V}O_3$ [88–90]	$NaM^{V}F_6$, M = Mo,W [91,92]
(j)	$U^{III/IV}M^{V/IV}C_2$[a], M = Mn,Tc,Re [2]	$Li_7Mn^{V}N_4$, $Sr_{6.75}Re^{V}_{1.25}N_7O_{0.125}$ [77,93]	$K_{0.48}Mn^{V}_{1.94}O_{5.18}$, $LiRe^{V}O_3$ [94,95]	$CsRe^{V}F_6$ [96]
(k)			$Ag_3Ru^{V}O_4$, $NdOs^{V}O_4$ [97,98]	$KM^{V}F_6$, M = Ru,Os [99,100]
(l)			$K_3Co^{V}O_4$, $Pr_3Ir^{V}O_7$ [76,101]	
(m)				$KPt^{V}F_6$ [102]
(n)		$La_3Nb_2^{IV}N_6$, $Li_2Ta_2^{IV}N_4$ [103,104]	$BaM^{IV}O_3$, M = V,Nb,Ta [105–107]	$Cs_2M^{IV}F_6$, M = V,Nb [108,109]
(o)			$Na_2Cr^{IV}O_3$, $SrMo^{IV}O_3$ [110,111]	$BaCr^{IV}F_6$, $Li_2Mo^{IV}F_6$ [112,113]
(p)		$Li_6Ca_2Mn_2^{IV}N_6$ [114]	$CaMn^{IV}O_3$, $Li_2Re^{IV}O_3$ [115,116]	$K_2M^{IV}F_6$, M = Mn,Tc,Re [117–119]
(q)			$BaFe^{IV}O_3$, $Na_2Ru^{IV}O_3$, $BaOs^{IV}O_3$ [120–122]	
(r)			$BaCo^{IV}O_3$, $Sr_3Rh_2^{IV}O_7$, $Ca_4Ir^{IV}O_6$ [123–125]	$K_2Co^{IV}F_6$, $Li_2M^{IV}F_6$ M = Rh,Ir [126-128]
(s)			$BaNi^{IV}O_3$, $Li_2Pd^{IV}O_3$ $Ca_4Pt^{IV}O_6$ [129–131]	$K_2Ni^{IV}F_6$, $Cs_2Pt^{IV}F_6$ $BaPd^{IV}F_6$ [132–134]
(t)		$Ca_3V^{III}N_3$ [135]	$LaV^{III}O_3$, $LaNb_7^{III}O_{12}$ [136,137]	$NaV^{III}F_4$, $Hg_3M^{III}F_6$, M = Nb,Ta [138-140]
(u)	$Ho_2M_2^{III}C_3$, M = Cr,Mo [2,9]	$Ca_3Cr^{III}N_3$ [141]	$DyMn^{III}O_3$, $LiMo^{III}O_2$ [142,143]	$Li_3Cr^{III}F_6$, $K_3M^{III}F_6$, M = Mo,W [92,144,145]
(v)		$Ce_2Mn^{III}N_3$ [146]	$LiMn^{III}O_2$ [147]	$Na_2Mn^{III}F_5$ [148]
(w)		$Ba_3Fe^{III}N_3$[149]	$Li(Co_{1-x}Fe^{III}{}_x)O_2$, $NaRu^{III}O_2$ [150,151]	$CaFe^{III}F_5$ [152]

Table 4 (*continued*)

Label	Carbon	Nitrogen	Oxygen	Fluorine
(x)			$LaCo^{III}O_3$, $LiRh^{III}O_3$ [153,154]	$CsCo^{III}F_4$, $Sr_2Rh^{III}F_7$ [155,156]
(y)			$NaNi^{III}O_2$, $LaPd^{III}O_3$, $PbPt_2^{III}O_4$ [157–159]	$Na_3Ni^{III}F_6$ [160]
(z)				$NaV^{II}F_3$ [161]
(aa)	$Pr_2M^{II}C_2$, M = Mo,W [12,13]			$KCr^{II}F_3$ [162]
(ab)	$Pr_2Re^{II}C2$ [14]		$BaMn_2^{II}O_3$ [163]	$KMn^{II}F_3$ [164]
(ac)	$Gd_2Os^{II}C_2$ [15]	$Li_4Fe^{II}N_2$ [60]	$Na_4Fe^{II}O_3$ [165]	$NaFe^{II}F_3$ [166]
(ad)			$K_4Co_2^{II}O_4$ [167]	$NaCo^{II}F_3$ [168]
(ae)			$Ag_2Ni^{II}O_2$, $Li_2Pd^{II}O_2$, $Na_2Pt^{II}O_3$ [169-171]	$NaM^{II}F_3$, M = Ni,Pd [168,172]
(af)		$Ce_2Cr^{I}N_3$ [173]		
(ag)		$Li_2[(Li_{1-x}Mn^{I}_x)N]$ [174]		
(ah)		$Li_2[(Li_{1-x}Fe^{I}_x)N]$ [56]	$K_3Fe^{I}O_2$ [175]	
(ai)	$YCo^{I}C$ [18]	$(Li,Co^{I})_3N$ [176]	$Rb_3Co^{I}O_2$ [177]	
(aj)		$(Li,Ni^{I})_3N$ [176]	$NdNi^{I}O_{2+x}$ [178]	
(ak)		$Ba_2(Ni_3^{0/I})N_2$ [57]		
(al)	$Th_2^{IV}M^{0}C_2$ M = Ru,Os [17]			
(am)	$Th_2^{IV}Rh^{0}C_2$, $U_2^{IV}Ir^{0}C_2$ [16,17]			
(an)	$Th_2^{IV}M^{0}C_2$ M = Ni,Pt [17]			

[a]The oxidation state of the uranium atoms in their respective compounds is probably mixed or intermediate III/IV, as is frequently the case for uranium compounds with similar composition [39].

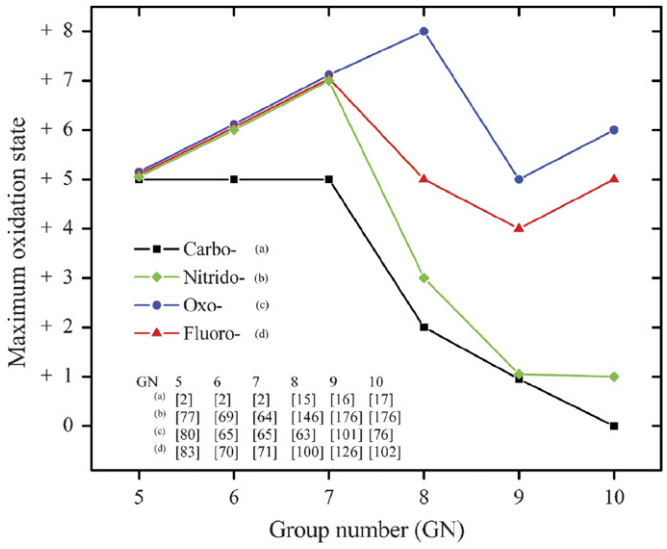

Fig. 12. Maximum oxidation states of group 5 to 10 metals in carbo-, nitrido-, oxo-, and fluorometalates.

homogeneity ranges; (ii) the crystal structures contain from a structural point of view specific polyanions $[T_yC_z]^{n-}$, ranging from discrete units, chains, layers to three-dimensional networks; (iii) the polyanions as structural entities contain the T–C bonds as the strongest covalent interactions; (iv) in contrast, the chemical bonding situation in the metal-rich carbides is dominated by metal–metal interactions outweighing the still strong T–C interactions simply by their large number; (v) carbometalates extend naturally the sequence of complex anions from fluoro-, oxo-, and nitridometalates.

The concept of carbometalates has of course its limitations: (i) in the case of an unpredictable oxidation state of the A species or due to increased metal–metal interactions the assignment of charge to the polyanion is difficult; (ii) in the case of metal to carbon ratios close to 2 or 4 the outcome, i.e., the structural chemistry is unpredictable; (iii) even for ideal carbometalates there may be significant distortions of the $[T_yC_z]^{n-}$ polyhedra due to A–T and T–T interactions. The main benefit of the presented classification of ternary carbides into metal-rich carbides and carbometalates is probably its strategic help. Novel carbometalates may be synthesized in a targeted approach and structural information, e.g. the coordination polyhedra of the transition metals and their linkages can be anticipated.

References

[1] D.T. Cromer, A.C. Larson, R.B. Roof Jr., Acta Crystallogr. 17 (1964) 272–276.
[2] W. Jeitschko, R.K. Behrens, Z. Metallk. 77 (1986) 788–793.
[3] G. Block, W. Jeitschko, Monatsh. Chem. 119 (1988) 319–326.
[4] R.K. Behrens, W. Jeitschko, Monatsh. Chem. 118 (1987) 43–50.
[5] M.M. Khalili, O.I. Bodak, E.P. Marusin, A.O. Pecharskaya, Kristallografiya 35 (1990) 337–341.
[6] R.K. Behrens, W. Jeitschko, J. Less-Common Met. 160 (1990) 185–192.
[7] K. Zeppenfeld, R. Pöttgen, M. Reehuis, W. Jeitschko, R.K. Behrens, J. Phys. Chem. Solids 54 (1993) 257–261.
[8] E. Dashjav, W. Schnelle, F.R. Wagner, G. Kreiner, R. Kniep, Z. Anorg. Allg. Chem. 632 (2006) 2094.

[9] M. Reehuis, M. Gerdes, W. Jeitschko, B. Ouladdiaf, T. Stüsser, J. Magn. Magn. Mater. 195 (1999) 657–666.
[10] E. Dashjav, W. Schnelle, G. Kreiner, R. Kniep, Z. Kristallogr. NCS 220 (2005) 129–130.
[11] E. Dashjav, G. Kreiner, W. Schnelle, F.R. Wagner, R. Kniep, Z. Anorg. Allg. Chem. 630 (2004) 2277–2286.
[12] E. Dashjav, G. Kreiner, W. Schnelle, F.R. Wagner, R. Kniep, Z. Anorg. Allg. Chem. 630 (2004) 689–696.
[13] E. Dashjav, G. Kreiner, F.R. Wagner, W. Schnelle, R. Kniep, Z. Anorg. Allg. Chem. 630 (2004) 1716.
[14] W. Jeitschko, G. Block, G.E. Kahnert, R.K. Behrens, J. Solid State Chem. 89 (1990) 191–201.
[15] M.H. Gerdes, W. Jeitschko, K.H. Wachtmann, M.E. Danebrock, J. Mater. Chem. 7 (1997) 2427–2431.
[16] A.L. Bowman, G.P. Arnold, N.H. Krikorian, W.H. Zachariasen, Acta Crystallogr. B27 (1971) 1067–1068.
[17] M.A. Moss, W. Jeitschko, Z. Anorg. Allg. Chem. 603 (1991) 57–67.
[18] M.H. Gerss, W. Jeitschko, Z. Naturforsch. B: Chem. Sci. 41 (1986) 946–950.
[19] M.E. Danebrock, W. Jeitschko, A.M. Witte, R. Pöttgen, J. Phys. Chem. Solids 56 (1995) 807–811.
[20] K.H. Wachtmann, T. Hüfken, W. Jeitschko, J. Solid State Chem. 131 (1997) 49–53.
[21] K.H. Wachtmann, M.A. Moss, R.D. Hoffmann, W. Jeitschko, J. Alloys Compd. 219 (1995) 279–284.
[22] H. Hollek, Binäre und ternäre Carbid- und Nitridsysteme der Übergangsmetalle, Bornträger, Berlin, 1984.
[23] W. Jeitschko, G. Block, Z. Anorg. Allg. Chem. 528 (1985) 61–68.
[24] O. Isnard, J.L. Soubeyroux, D. Fruchart, T.H. Jacobs, K.H.J. Buschow, J. Phys.: Condens. Matter 4 (1992) 6367–6374.
[25] G. Block, W. Jeitschko, Inorg. Chem. 25 (1986) 279–282.
[26] G. Block, W. Jeitschko, J. Solid State Chem. 70 (1987) 271–280.
[27] W.G. Haije, T.H. Jacobs, K.H.J. Buschow, J. Less-Common Met. 163 (1990) 353–359.
[28] R. Pöttgen, W. Jeitschko, C. Evers, M.A. Moss, J. Alloys Compd. 186 (1992) 223–232.
[29] O.I. Bodak, E.P. Marusin, V.S. Fundamensky, V.A. Bruskov, Kristallografiya 27 (1982) 1098–1101.
[30] A.A. Putyatin, O.V. Makarova, Inorg. Mater. 27 (1991) 333–337.
[31] M.M. Khalili, O.I. Bodak, E.P. Marusin, A.O. Pecharskaya, Kristallografiya 35 (1990) 1378–1380.
[32] M.A. Moss, W. Jeitschko, J. Alloys Compd. 182 (1992) 157–164.
[33] A.A. Putyatin, L.G. Sevastyanova, Vestn. Mosk. Univ.—Ser. 2: Khim. 28 (1987) 199.
[34] M. Gueramian, A. Bezinge, K. Yvon, J. Muller, Solid State Commun. 64 (1987) 639–644.
[35] J.F. Herbst, J.J. Croat, F.E. Pinkerton, W.B. Yelon, Phys. Rev. B 29 (1984) 4176–4178.
[36] C. Hellwig, K. Girgis, J. Schefer, K.H.J. Buschow, P. Fischer, J. Less-Common Met. 169 (1991) 147–156.
[37] C.J.M. Denissen, B.D. Demooij, K.H.J. Buschow, J. Less-Common Met. 139 (1988) 291–298.
[38] J. Lima-De-Faria, E. Hellner, F. Liebau, E. Makovicky, E. Parthé, Acta Crystallogr. A 46 (1990) 1–11.
[39] T. Vomhof, R. Pöttgen, W. Jeitschko, J. Alloys Compd. 196 (1993) 173–176.
[40] M.J. Sanderson, N.C. Baenziger, Acta Crystallogr. 6 (1953) 627–631.
[41] E.S. Makarov, I.S. Vinagradova, Kristallografiya 1 (1956) 511–515.
[42] J.V. Florio, N.C. Baenziger, R.E. Rundle, Acta Crystallogr. 9 (1956) 367–372.
[43] R.B. King, Russian Chem. Bull. 42 (1993) 1283–1291.
[44] R.B. King, J. Organomet. Chem. 536 (1997) 7–15.
[45] R.B. King, J. Indian Chem. Soc. 77 (2000) 603–607.
[46] R. Hoffmann, J. Li, R.A. Wheeler, J. Am. Chem. Soc. 109 (1987) 6600–6602.
[47] H. Deng, R. Hoffmann, Inorg. Chem. 32 (1993) 1991–1996.
[48] H.J. Koo, M.H. Whangbo, Inorg. Chem. 38 (1999) 2204–2210.
[49] G. Krier, O. Jepsen, A. Burkhard, O.K. Andersen, A Tight Binding LMTO-ASA Program, Version 4.7, Stuttgart, Germany, 1998.
[50] O. Jepsen, O.K. Andersen, Z. Phys. B—Condens. Matter 97 (1995) 35–47.
[51] W.R.L. Lambrecht, O.K. Andersen, Phys. Rev. B 34 (1986) 2439–2449.
[52] R. Dronskowski, P.E. Blöchl, J. Phys. Chem. 97 (1993) 8617–8624.
[53] R. Kniep, Pure Appl. Chem. 69 (1997) 185–191.
[54] P. Höhn, R. Kniep, Z. Anorg. Allg. Chem. 628 (2002) 463–467.
[55] R. Niewa, Z.L. Huang, W. Schnelle, Z. Hu, R. Kniep, Z. Anorg. Allg. Chem. 629 (2003) 1778–1786.
[56] J. Klatyk, W. Schnelle, F.R. Wagner, R. Niewa, P. Novak, R. Kniep, M. Waldeck, V. Ksenofontov, P. Gütlich, Phys. Rev. Lett. 88 (2002) 207202-1–207202-4.
[57] A. Mehta, P. Höhn, W. Schnelle, V. Petzold, H. Rosner, U. Burkhardt, R. Kniep, Chem.-A Eur. J. 12 (2006) 1667–1676.
[58] U. Ruschewitz, Coord. Chem. Rev. 244 (2003) 115–136.
[59] U. Ruschewitz, Z. Anorg. Allg. Chem. 632 (2006) 705–719.
[60] A. Gudat, R. Kniep, A. Rabenau, Angew. Chem. Int. Ed. 30 (1991) 199–200.
[61] M.Y. Chern, F.J. Disalvo, J. Solid State Chem. 88 (1990) 459–464.
[62] A. Gudat, R. Kniep, J. Maier, J. Alloys Compd. 186 (1992) 339–345.
[63] K.M. Mogare, W. Klein, M. Jansen, Z. Anorg. Allg. Chem. 631 (2005) 468–471.
[64] A. Chaushli, H. Jacobs, U. Weisser, J. Strähle, Z. Anorg. Allg. Chem. 626 (2000) 1909–1914.
[65] A.F. Hollemann, E. Wiberg, Lehrbuch der Anorganischen Chemie, Walter de Gruyter, Berlin, New York, 1995.
[66] I.C. Hwang, K. Seppelt, J. Fluorine Chem. 102 (2000) 69–72.
[67] M.D. Silverman, H.A. Levy, J. Am. Chem. Soc. 76 (1954) 3317–3319.
[68] W. Levason, M. Tajik, M. Webster, J. Chem. Soc.—Dalton Trans. (1985) 1735–1736.
[69] A. Gudat, S. Haag, R. Kniep, A. Rabenau, Z. Naturforsch. A: Phys. Sci. 45 (1990) 111–120.
[70] S. Giese, K. Seppelt, Angew. Chem.—Int. Ed. 33 (1994) 461–463.
[71] O. Hochrein, R. Kniep, Z. Anorg. Allg. Chem. 627 (2001) 301–303.
[72] P.A. Koz'min, Zh. Strukt. Khim. (1964) 70–76.
[73] M.L. Hoppe, E.O. Schlemper, R.K. Murmann, Acta Crystallogr. B38 (1982) 2237–2239.
[74] M. Shikano, R.K. Kremer, M. Ahrens, H.J. Koo, M.H. Whangbo, J. Darriet, Inorg. Chem. 43 (2004) 5–7.
[75] C.R. Bavay Tridot, C.R. Acad. Sci. Ser. II C 276 (1973) 1025.
[76] R. Hoppe, Angew. Chem.—Int. Ed. 20 (1981) 62–87.
[77] R. Juza, W. Gieren, J. Haug, Z. Anorg. Allg. Chem. 300 (1959) 61–71.
[78] D.A. Vennos, F.J. Disalvo, Acta Crystallogr. C48 (1992) 610–612.
[79] C. Wachsmann, H. Jacobs, J. Alloys Compd. 190 (1992) 113–116.
[80] K. Kato, E. Takayama, Acta Crystallogr. B 40 (1984) 102–105.
[81] V.K. Trunov, V.A. Efremov, Y.A. Velikodnyi, I.M. Averina, Kristallografiya 26 (1981) 67–71.
[82] G.M. Wolten, Acta Crystallogr. 23 (1967) 939–944.
[83] J.L. Hoard, J. Am. Chem. Soc. 61 (1939) 1252–1259.
[84] R.B. English, A.M. Heyns, E.C. Reynhardt, J. Phys. C: Solid State Phys. 16 (1983) 829–840.
[85] A. Tennstedt, R. Kniep, M. Huber, W. Haase, Z. Anorg. Allg. Chem. 621 (1995) 511–515.
[86] S.H. Elder, L.H. Doerrer, F.J. Disalvo, J.B. Parise, D. Guyomard, J.M. Tarascon, Chem. Mater. 4 (1992) 928–937.
[87] S. Kaskel, D. Hohlwein, J. Strähle, J. Solid State Chem. 138 (1998) 154–159.
[88] R. Saez-Puche, E. Jimenez, J. Isasi, M.T. Fernandez-Diaz, J.L. Garcia-Munoz, J. Solid State Chem. 171 (2003) 161–169.
[89] P. Gall, P. Gougeon, Acta Crystallogr.—Section C 61 (2005) 169–170.
[90] C.N.W. Darlington, J.A. Hriljac, K.S. Knight, Acta Crystallogr. B 59 (2003) 584–587.
[91] A.J. Edwards, R.D. Peacock, J. Chem. Soc. (1961) 4253–4254.

[92] S.E. Eklund, J.Q. Chambers, G. Mamantov, J. Diminnie, C.E. Barnes, Inorg. Chem. 40 (2001) 715–722.
[93] R. Karam, R. Ward, Inorg. Chem. 9 (1970) 1849–1852.
[94] A.C. Gaillot, D. Flot, V.A. Drits, A. Manceau, M. Burghammer, B. Lanson, Chem. Mater. 15 (2003) 4666–4678.
[95] R.J. Cava, A. Santoro, D.W. Murphy, S. Zahurak, R.S. Roth, J. Solid State Chem. 42 (1982) 251–262.
[96] B.F. Hoskins, A. Linden, P.C. Mulvaney, T.A. Odonnell, Inorg. Chim. Acta 88 (1984) 217–222.
[97] W. Klein, M. Jansen, Acta Crystallogr. C 61 (2005) I1–I2.
[98] F. Abraham, J. Trehoux, D. Thomas, J. Inorg. Nucl. Chem. 42 (1980) 1627–1630.
[99] E. Weise, W. Klemm, Z. Anorg. Allg. Chem. 279 (1955) 74–85.
[100] M.A. Hepworth, K.H. Jack, G.J. Westland, J. Inorg. Nucl. Chem. 2 (1956) 79–87.
[101] J.F. Vente, D.J.W. Ijdo, Mater. Res. Bull. 26 (1991) 1255–1262.
[102] N. Bartlett, D.H. Lohmann, J. Chem. Soc. (1964) 619–627.
[103] L. Cario, Z.A. Gal, T.P. Braun, F.J. Disalvo, B. Blaschkowski, H.J. Meyer, J. Solid State Chem. 162 (2001) 90–95.
[104] T. Brokamp, H. Jacobs, J. Alloys Compd. 183 (1992) 325–344.
[105] G. Liu, J.E. Greedan, J. Solid State Chem. 110 (1994) 274–289.
[106] Y. Grin, H. Müller-Buschbaum, H.G. von Schnering, Z. Naturforsch. B: Chem. Sci. 52 (1997) 153–156.
[107] A. Ritter, T. Lydssan, B. Harbrecht, Z. Anorg. Allg. Chem. 624 (1998) 1791–1795.
[108] K. Walterss, K.A. Wilhelmi, A. Carpy, J. Galy, Bull. Soc. Fr. Miner. Crystallogr. 97 (1974) 13–17.
[109] J. Chassaing, M.B. Debournonville, D. Bizot, M. Quarton, Eur. J. Solid State Inorg. Chem. 28 (1991) 441–451.
[110] C.C. Addison, M.G. Barker, J. Chem. Soc. (1965) 5534–5537.
[111] G. Liu, X.H. Zhao, H.A. Eick, J. Alloys Compd. 187 (1992) 145–156.
[112] G. Siebert, R. Hoppe, Z. Anorg. Allg. Chem. 391 (1972) 126–136.
[113] W.H. Baur, Acta Crystallogr.—Section B 50 (1994) 141–146.
[114] O. Hochrein, Y. Grin, R. Kniep, Angew. Chem.—Int. Ed. 37 (1998) 1582–1585.
[115] M.E.M. Jorge, A.C. dos Santos, M.R. Nunes, Int. J. Inorg. Mater. 3 (2001) 915–921.
[116] E. Hartmann, Mineral.-Petrographisches Institut, Universität Heidelberg, FRG., ICDD Grant-in-Aid, 1990.
[117] P. Bukovec, R. Hoppe, J. Fluorine Chem. 23 (1983) 579–587.
[118] K. Schwochau, Z. Naturforsch. A: Phys. Sci. A 19 (1964) 1237–1241.
[119] G.R. Clark, D.R. Russell, Acta Crystallogr. B 34 (1978) 894–895.
[120] M. Zanne, C. Gleitzer, Bull. Soc. Chim. Fr. (1971) 1567.
[121] K.M. Mogare, K. Friese, W. Klein, M. Jansen, Z. Anorg. Allg. Chem. 630 (2004) 547–552.
[122] R.F. Sarkozy, B.L. Chamberland, Mater. Res. Bull. 8 (1973) 1351–1359.
[123] C. Felser, K. Yamaura, R.J. Cava, J. Solid State Chem. 146 (1999) 411–417.
[124] K. Yamaura, Q. Huang, D.P. Young, Y. Noguchi, E. Takayama-Muromachi, Phys. Rev. B 66 (2002).
[125] M.J. Davis, M.D. Smith, H.C. zur Loye, Acta Crystallogr. C 57 (2001) 1234–1236.
[126] J.W. Quail, G.A. Rivett, Can. J. Chem. 50 (1972) 2447–2450.
[127] V. Wilhelm, R. Hoppe, Z. Anorg. Allg. Chem. 405 (1974) 193–196.
[128] H. Fitz, B.G. Müller, O. Graudejus, N. Bartlett, Z. Anorg. Allg. Chem. 628 (2002) 133–137.
[129] H. Krischner, K. Torkar, B.O. Kolbesen, J. Solid State Chem. 3 (1971) 349–357.
[130] Y. Laligant, P. Lacorre, J. Rodriquez-Carvajal, Mater. Sci. Forum 378-3 (2001) 632–637.
[131] J.B. Claridge, R.C. Layland, H.C. zur Loye, Acta Crystallogr. C 53 (1997) 1740–1741.
[132] J.C. Taylor, P.W. Wilson, J. Inorg. Nucl. Chem. 36 (1974) 1561–1563.
[133] M. Bork, R. Hoppe, Z. Anorg. Allg. Chem. 622 (1996) 417–424.
[134] C. De Nadai, A. Demourgues, P. Gravereau, J. Grannec, J. Solid State Chem. 148 (1999) 242–249.
[135] D.A. Vennos, F.J. Disalvo, J. Solid State Chem. 98 (1992) 318–322.
[136] H. Seim, H. Fjellvag, B.C. Hauback, Acta Chem. Scand. 52 (1998) 1301–1306.
[137] J. Xu, T. Emge, M. Greenblatt, J. Solid State Chem. 123 (1996) 21–29.
[138] B. Peschel, D. Babel, Z. Anorg. Allg. Chem. 623 (1997) 1614–1620.
[139] I.D. Brown, R.J. Gillespie, K.R. Morgan, Z. Tun, P.K. Ummat, Inorg. Chem. 23 (1984) 4506–4508.
[140] A. Boukhari, J.P. Chaminade, M. Pouchard, M. Vlasse, Acta Crystallogr. B 36 (1980) 237–240.
[141] D.A. Vennos, M.E. Badding, F.J. Disalvo, Inorg. Chem. 29 (1990) 4059–4062.
[142] N. Kamegashira, H. Satoh, S. Ashizuka, Mater. Sci. Forum 449–4 (2004) 1045–1048.
[143] L.E. Aleandri, R.E. Mccarley, Inorg. Chem. 27 (1988) 1041–1044.
[144] A.K. Tyagi, J. Kohler, Mater. Res. Bull. 35 (2000) 135–141.
[145] L.M. Toth, G.D. Brunton, G.P. Smith, Inorg. Chem. 8 (1969) 2694–2697.
[146] R. Niewa, G.V. Vajenine, F.J. Disalvo, H.H. Luo, W.B. Yelon, Z. Naturforsch. A: Phys. Sci. 53 (1998) 63–74.
[147] J. Akimoto, Y. Takahashi, Y. Gotoh, K. Kawaguchi, K. Dokko, I. Uchida, Chem. Mater. 15 (2003) 2984–2990.
[148] S. Carlson, Y. Xu, R. Norrestam, Z. Kristallogr. 214 (1999) 259–263.
[149] P. Höhn, R. Kniep, A. Rabenau, Z. Kristallogr. 196 (1991) 153–158.
[150] M. Holzapfel, C. Haak, A. Ott, J. Solid State Chem. 156 (2001) 470–479.
[151] M. Shikano, C. Delmas, J. Darriet, Inorg. Chem. 43 (2004) 1214–1216.
[152] J. Graulich, W. Massa, D. Babel, Z. Anorg. Allg. Chem. 629 (2003) 365–367.
[153] O. Haas, R.P.W.J. Struis, J.M. McBreen, J. Solid State Chem. 177 (2004) 1000–1010.
[154] K. Hobbie, R. Hoppe, Z. Anorg. Allg. Chem. 535 (1986) 20–30.
[155] P. Lacorre, J. Pannetier, T. Fleischer, R. Hoppe, G. Ferey, J. Solid State Chem. 93 (1991) 37–45.
[156] R. Domesle, R. Hoppe, Z. Anorg. Allg. Chem. 501 (1983) 102–110.
[157] M. Sofin, M. Jansen, Z. Naturforsch. B: Chem. Sci. 60 (2005) 701–704.
[158] S.J. Kim, S. Lemaux, G. Demazeau, J.Y. Kim, J.H. Choy, J. Am. Chem. Soc. 123 (2001) 10413–10414.
[159] N. Tancret, S. Obbade, N. Bettahar, F. Abraham, J. Solid State Chem. 124 (1996) 309–318.
[160] H. Henkel, R. Hoppe, Z. Anorg. Allg. Chem. 364 (1969) 253–260.
[161] R.F. Williamson, W.O.J. Boo, Inorg. Chem. 16 (1977) 646–648.
[162] A.J. Edwards, R.D. Peacock, J. Chem. Soc. (1959) 4126–4127.
[163] K. Sander, H. Müller-Buschbaum, Z. Anorg. Allg. Chem. 451 (1979) 35–39.
[164] J. Kapusta, P. Daniel, A. Ratuszna, Phys. Rev. B 59 (1999) 14235–14245.
[165] H. Rieck, R. Hoppe, Naturwissenschaften 61 (1974) 126–127.
[166] G. Benner, R. Hoppe, J. Fluorine Chem. 46 (1990) 283–295.
[167] F. Bernhardt, R. Hoppe, Z. Anorg. Allg. Chem. 620 (1994) 586–591.
[168] B. Lütgert, D. Babel, Z. Anorg. Allg. Chem. 616 (1992) 133–140.
[169] M. Schreyer, M. Jansen, Angew. Chem.—Int. Ed. 41 (2002) 643–646.
[170] R. Wolf, R. Hoppe, Z. Anorg. Allg. Chem. 536 (1986) 77–80.
[171] W. Urland, R. Hoppe, Z. Anorg. Allg. Chem. 392 (1972) 23–26.
[172] B. Bachmann, B.G. Müller, Z. Anorg. Allg. Chem. 619 (1993) 387–391.
[173] S. Broll, W. Jeitschko, Z. Naturforsch. B: Chem. Sci. 50 (1995) 905–912.
[174] R. Niewa, F.R. Wagner, W. Schnelle, O. Hochrein, R. Kniep, Inorg. Chem. 40 (2001) 5215–5222.
[175] F. Bernhardt, R. Hoppe, Z. Anorg. Allg. Chem. 619 (1993) 969–975.
[176] R. Juza, W. Sachsze, Z. Anorg. Chem. 253 (1945) 95–108.
[177] M. Sofin, M. Jansen, Z. Anorg. Allg. Chem. 627 (2001) 2115–2117.
[178] M.A. Hayward, M.J. Rosseinsky, Solid State Sci. 5 (2003) 839–850.
[179] A. Gudat, P. Höhn, R. Kniep, A. Rabenau, Z. Naturforsch. B: Chem. Sci. 46 (1991) 566–572.